ATG13 Gene Expression in Post-Infectious Syndrome Patients

BY

Rachel Mae Sokyrka

A thesis submitted to the

Department of Biology

Mount Allison University

in partial fulfilment of the requirements for the

Bachelor of Science degree with Honours

April 9, 2024

Acknowledgements

I would first like to extend my greatest thanks and sincere gratitude to Dr. Lloyd for not only supervising my honours project but inspiring me and sparking my love for research. Thank you for supporting me, providing answers to my many questions, offering me guidance in my writing and presentation skills, and overall giving me the opportunity to truly experience the wonders of science.

I would like to express a special thanks of gratitude to Anne Berthold for training me in the basis of my lab techniques, being a beacon of knowledge throughout my time working for Geneticks, providing me mentorship on my independent study and honours work, teaching me how to become a better presenter, and for being a true friend.

I would like to thank Samantha Bishop for answering my questions, handling my samples, and taking care of the 'behind the scenes'.

I would like to extend my thanks to Dr. Crosby for taking the time to be my second reader and providing valued and appreciated feedback. I would also like to thank Dr. Riley for giving me guidance and support with current advances, statistics, and RStudio - my stats wouldn't be here without you!

Thank you to all my lab members for inspiring me, helping me, and providing friendship throughout my two years in the Lloyd lab, and beyond. Charmaine, thank you for your guidance with immunohistochemistry. Lauren, thank you for teaching me RNA extraction. Jaclyn and Grace, I truly appreciate and value our friendship in and out of the lab. Thank you for making my Sackville summer filled with laughter and adventure, spending late nights studying, early mornings walking to class together, and being the greatest 'coworkers' anyone could ask for.

Andi, thank you for being the most supportive roommate and friend, encouraging me through life's challenges and celebrating our successes and accomplishments. Tyler, thank you for being there for me no matter what, having the utmost patience for allowing me to practice presenting my honours to you. I would also like to thank the rest of my friends for their unwavering support and memories throughout my time at Mount Allison. Thank you to my fellow honours students who continue to inspire and motivate me.

Finally, thank you to my family, especially my mom and dad. I cannot begin to thank you enough for inspiring me to work hard and never give up on my dreams. Thank you for showing me what it means to have determination and perseverance. I would not be the person I am without your love and support.

Table of Contents

List of Tables

List of Figures

Abstract

Post-infectious syndromes are unexplained failure in recovering from an infection, leading to a variety of chronic symptoms. These chronic illnesses are poorly understood. Our study aims to determine *ATG13* gene expression in post-infectious syndrome participants. The *ATG13* gene is responsible for autophagy, immune function, the stress response, and oncogenesis. A connection between Chronic Fatigue Syndrome and *ATG13* gene expression was found in a recent study by Gottschalk and colleagues (2022), but a real-world sample was required to determine significance of these results. Blood samples for our study were collected from healthy participants and post-infectious syndrome participants including Chronic Fatigue Syndrome, multiple sclerosis, fibromyalgia, diagnosed Lyme disease, probable Lyme disease, and possible Lyme disease. Sera collected from the blood of the participants was used for enzyme-linked immunosorbent assays (ELISAs) to quantify the amount of ATG13 present in the sera of each participant, testing duplicates of each sample. ATG13 was found to be under expressed in multiple sclerosis and treated, fully recovered Lyme disease participants, indicating that ATG13 is likely involved in these conditions. Immunohistochemistry was used to visualize ATG13 protein in brain slices. Two slices from a deceased human participant with a concussion were used, one as a negative technical control and the other as a negative biological control. A third slice from a deceased human participant with Lyme disease was used as a positive control. Abundant fluorescence was observed in the positive control, minimal fluorescence was observed in the negative biological control, and no fluorescence was observed in the negative technical control, suggesting that ATG13 may function differently in the participant with Lyme disease. To examine *ATG13* gene regulation, the *ATG13* gene sequence was submitted to a transcription factor sequence binding site search tool and a cluster of the AP-1 transcription factor binding sites were found, suggesting that it could be a potential regulator of ATG13. This study contributes to further the knowledge of poorly understood chronic illness and provides potential information for testing, treatment, and diagnosis of these debilitating conditions.

Introduction

1.1 Post-infectious syndrome background

Humans have a close relationship with microbes (Drexler & Medicine (US), 2010). Certain microbes inhabit various places in and on our bodies, including the gut, the skin, and mucous membranes, each with specific functions to keep us healthy, such as protection from disease and aiding in digestion (Drexler & Medicine (US), 2010). Although human bodies require certain microbes to stay alive, infection from other microbes can cause sickness, or even death (Drexler & Medicine (US), 2010). For millions of years, infections from viruses, bacteria or other microbes have been impacting human populations, and remain prevalent in the world today (Wolfe et al., 2012). Some common modern infections are Covid-19, the common cold, the stomach flu, among countless other disease causing-infections (Poenaru et al., 2021). With the ongoing advancements in medicine, and most importantly our immune systems, these infections are quickly cleared in the body (Poenaru et al., 2021). Although infections are commonly cleared, sometimes illness persists in individuals, lasting from several months up to many years, and in some cases, individuals do not recover (Poenaru et al., 2021). These prolonged symptoms are termed 'post-infectious syndromes' (Poenaru et al., 2021). Post-infectious syndromes are an unexplained failure in recovering from an infection, leading to continuous symptoms such as persistent cognitive or muscle fatigue, muscle pain, other flu-like symptoms, or much more serious life-threatening symptoms which can lead to death (Choutka et al., 2022). Examples of post-infectious syndromes include long covid, Chronic Fatigue Syndrome, chronic Lyme disease, fibromyalgia, and multiple sclerosis (Choutka et al., 2022). There are three broad causes of post-infectious syndromes: pathogen persistence, damage, and immune dysregulation (Sherif et al., n.d.). Although the broad causes of post-infectious syndromes are known, differentiating between these causes is critical to allow for therapeutic approaches, which are not yet identified.

1.2 Post-infectious syndrome examples

Covid-19, caused by SARS-CoV-2 infection, is a pandemic causing immense mortality and morbidity among populations all over the globe, leaving many individuals with persisting, long lasting symptoms termed 'long covid' (Raveendran et al., 2021). The persisting symptoms can be experienced during the initial Covid-19 infection, or they can be new (Raveendran et al., 2021). Common symptoms include fatigue, headaches, complaints within the upper respiratory system, fever, and gastrointestinal complaints (Raveendran et al., 2021). Patients experiencing long covid post-infectious symptoms usually test negative with a PCR test for SARS-CoV-2, suggesting that microbiologically, they are cleared or healed from SARS-CoV-2 and the viral load is low or absent, but clinical recovery has not occurred (Raveendran et al., 2021). Diagnosing long covid patients comes with many challenges as there are multiple symptoms, symptom duration, and severity of symptoms (Raveendran et al., 2021). Testing and diagnosis approaches have differed by country, and some individuals were either initially asymptomatic or did not have access to testing to support a diagnosis, which can lead to difficulty in diagnosing post-infectious syndromes later on (Raveendran et al., 2021). Some risk factors associated with developing long covid are increased age, sex (long covid being twice as common in females than males), more symptoms during the initial infection and comorbidities (Raveendran et al., 2021). The main treatment option for long covid is rehabilitation (Yong, 2021). This includes light aerobic exercise, breathing exercises, behavioural modification, and psychological support (Yong, 2021).

Chronic Lyme disease is another example of a post-infectious syndrome. This term describes patients with ongoing symptoms resulted from a current or previous infection with *Borrelia burgdorferi* (Wong et al., 2022) . Symptoms include joint pain, fatigue, swelling, negative impacts on memory or concentration, and speech problems (*Chronic Lyme Disease | NIAID*, 2018). There is much still unknown about Chronic Lyme Disease and some conflicting results on treatments and diagnosis, resulting in some researchers lack of support in this field (*Chronic Lyme Disease | NIH*, 2018). Diagnosing includes reviewing symptoms, recalling history of interaction with ticks, and blood tests looking for antibodies from the body fighting *Borrelia burgdorferi* (Bobe et al., 2021). Antibiotics are used to treat chronic Lyme disease but irreversible damage to the body may occur needing more than antibiotic treatment (Afari & Buchwald, 2003).

Fibromyalgia is a post-infectious syndrome that, unlike the previous examples, has an unknown cause. Suggested causes are stressful life events, genetic predisposition, and inflammatory and cognitive mechanisms (Sarzi-Puttini et al., 2020). Fibromyalgia patients have neurochemical imbalances in the central nervous system (Sarzi-Puttini et al., 2020). This causes central amplification of pain receptors identified by allodynia and hyperalgesia (Sarzi-Puttini et al., 2020). The disease affects people of all ages, but more common during middle ages, and is more prevalent in females (Siracusa et al., 2021). Various diseases often associated with fibromyalgia, including diabetes, infections, and psychiatric or neurological disorders (Siracusa et al., 2021). Common symptoms of fibromyalgia include chronic widespread pain, cognitive difficulties, physical exhaustion, anxiety, depression and sleep problems (Häuser et al., 2015). As with the other post-infectious syndromes, the pathogenesis of fibromyalgia still undetermined creating the difficulty of diagnosing this post-infectious syndrome (Siracusa et al., 2021). There are no current laboratory tests to diagnose fibromyalgia, but is currently diagnosed based by the collection of symptoms the patient experiences (Branch, 2017). Treatments include both pharmacological (anti-epileptic drugs, tricyclic antidepressants, serotonin reuptake inhibitors) and non-pharmacological methods (acupuncture, massage therapy, exercise) (Chinn et al., 2016).

Another post-infectious syndrome that is both growing in incidence and impacts many peoples across the globe, is multiple sclerosis (Dobson & Giovannoni, 2019). This is a chronic disease that impacts the central nervous system (Dobson & Giovannoni, 2019). Multiple sclerosis is due to the inflammation of gray and white matter tissues located in the central nervous system from focal immune cell infiltration (Ghasemi et al., 2017). There many known genes that increase risk of contracting multiple sclerosis (Dobson & Giovannoni, 2019). The main gene known for increased risk of multiple sclerosis is HLA-DRB1*15, which is a variant of the HLA-DRB1 gene that, in a normal case, helps the immune system distinguish the body's own proteins from foreign invaders including viruses (Dobson & Giovannoni, 2019). However, there are over 150 other single nucleotide polymorphisms that have been found to predispose people to multiple sclerosis (Dobson & Giovannoni, 2019). Along with genetic predisposition, there are some environmental factors that are thought to contribute, including smoking, obesity, vitamin D deficiency, and ultraviolet B light exposure (Dobson & Giovannoni, 2019). Smoking can increase the risk for multiple sclerosis by up to 50% (Dobson & Giovannoni, 2019). Multiple sclerosis is again more common in females with a ratio for prevalence of 3:1 for females versus males, but this is a recent change, as the prevalence was equal between males and females in the early 1900s (Dobson & Giovannoni, 2019). This may be due to females having an increase in vitamin D deficiency prevalence compared to males (Sellner et al., 2011). Symptoms of this disease include sensory disturbances, muscle weakness, speech difficulties, fatigue, bladder and bowel difficulties, vision impairment, dizziness and vertigo, and many more symptoms arising from neurological impairment (Ghasemi et al., 2017). Diagnosis includes review of medical history, magnetic resonance imaging, cerebral spinal fluid analysis, blood sample analysis, and evoked potentials (Ghasemi et al., 2017). Recent therapeutic strategies with success include B-cell targeted therapy which uses monoclonal antibodies to attack cells and slowing down nerve damage while alleviating inflammation (Faissner & Gold, 2019).

Chronic Fatigue Syndrome is a post-infectious syndrome defined by unrelenting fatigue that lasts at least 6 months and must significantly reduce the level of activity for the patient (Afari & Buchwald, 2003). To be categorized as Chronic Fatigue Syndrome, within 6 months, four or more symptoms must occur from the following list: sore throat, tender glands, memory or cognitive impairment, stiff or aching muscles, joint pain in multiple muscles, unrefreshing sleep, new headaches, and post exertional fatigue (Afari & Buchwald, 2003). Neuropsychiatric, infectious, and rheumatological co-morbidities can be linked with this illness (Afari & Buchwald, 2003). To be categorized as someone with Chronic Fatigue Syndrome, the patient must not have any other medical conditions that also may cause prolonged fatigue, including melancholic depression, eating disorders, substance use within 2 years of fatigue onset, bipolar disorders, or psychotic disorders (Afari & Buchwald, 2003). If a patient does not meet these specific requirements, they may also be diagnosed with idiopathic chronic fatigue (Afari & Buchwald, 2003). Although various mechanisms have been investigated including immunological, infections, psychiatric, sleep, and neuroendocrine mechanisms, a distinct etiology is still unknown (Afari & Buchwald, 2003). Chronic Fatigue Syndrome is mainly seen in patients aged 30-40, having a higher prevalence in females, as well as Latinos, African Americans, and Native Americans (Afari & Buchwald, 2003). It is common for comorbidities to happen, with functional illnesses being temporomandibular joint disorder, irritable bowel syndrome, fibromyalgia, and multiple chemical sensitivities (Afari & Buchwald, 2003). These conditions have overlapping clinical manifestations without a clear etiology and do not have unambiguous diagnostics, so people may get multiple diagnoses. Family and twin studies have been conducted to gain a better understanding of the genetic contributions to Chronic Fatigue Syndrome (Afari & Buchwald, 2003). These studies have found that a genetic predisposition as well as environmental factors may be factors, but limitations in the studies make firm conclusions premature (Holgate et al., 2011).

Overall, these post-infectious syndromes have chronic and debilitating effects on patients' lives all around the world. Many patients do not have access to healthcare necessary for these illnesses, and the impact of post-infectious syndromes has drastic impacts on the healthcare burden. Each post-infectious syndrome comes with a variety of hardships, leaving patients in serious pain and discomfort, along with the loss of ability for jobs and careers, self-care, and a normal daily life. Discovering underlying factors, such as gene expression, will aid in knowledge of post-infectious syndromes to better outcomes for patients in the future.

1.3 Post-infectious syndrome biomarker

Although not all people with a given infection develop a post-infectious syndrome, 10-30% of patients will end up with one. Understanding the biological factors that result in post-infectious syndromes is crucial for diagnosis and ideally treatment. This understanding has led to the search for disease biomarkers, which are used for disease screening, monitoring, characterization, and diagnosis (Aronson & Ferner, 2017).

A recent study by Gottschalk and colleagues reported evidence for such a biomarker for Chronic Fatigue Syndrome; they identified ATG13 over-expression in Chronic Fatigue Syndrome participants (Gottschalk et al., 2022). This study found an overexpression of the gene *ATG13* in Chronic Fatigue Syndrome participants, creating excitement and hope for other researchers and those suffering from this disease (Gottschalk et al., 2022).

The study started with two Chronic Fatigue Syndrome participants which were age-matched to control participants, then further validated this by seven more participants, matching age, sex, geographical location, and ethnicity (Gottschalk et al., 2022). The first two participants were used as a pilot study and the findings were supported by the next seven participants (Gottschalk et al., 2022). These participants were selectively chosen within the same clinic. The researchers estimated the protein aggregation propensities of serum samples and used a thioflavin T biochemical assay to test this (Gottschalk et al., 2022). They found that Chronic Fatigue Syndrome participants showed a significantly faster protein aggregation rate compared to healthy participants (Gottschalk et al., 2022). The increased protein aggregation suggests autophagy impairment (Gottschalk et al., 2022). Next, they looked at the upregulation of various autophagy markers in the serum from these participants, using ELISAs and antibody array assays (Gottschalk et al., 2022). The results showed that ATG13 could be dysregulated in Chronic Fatigue Syndrome participants (Gottschalk et al., 2022). Other genes were explored, finding an overexpression of ATG5, p62, and a-syn, although ATG13 had the greatest overexpression (Gottschalk et al., 2022). Next, they evaluated the lysosomal function in the participants finding some lysosomal proteases were upregulated while others were not significantly different (Gottschalk et al., 2022). Later, the researchers wanted to observe the microglial stress response, seeing if ATG13 had an effect (Gottschalk et al., 2022). They found this to be true, seeing that in microglial cells, serum-derived ATG13 was phosphorylated and causes the RAGE receptor to produce an oxidative stress response (Gottschalk et al., 2022).

This study had a sample size of only 9 age and sex-matched pairs from one region; the need for a larger and real-world sample population is clearly needed to evaluate this preliminary data. With the *ATG13* gene being connected to Chronic Fatigue Syndrome, this also allows for the idea that this gene could also be connected to other post-infectious syndromes.

Just as humans live and die, so do the cells in the body. The presence of cells in organisms requires ongoing cellular maintenance, which means removing or reusing damaged or dysfunctional parts of the cell. This cell cleaning process is termed autophagy and is the body's way of performing intracellular degradation (Kaizuka & Mizushima, 2016). There are many different genes responsible for autophagy and cellular maintenance, some of these are known as autophagy-related genes (ATG) (Kawamata et al., 2005). The pathogenesis of many known disorders can be caused by mutations to autophagy related genes, impairing autophagy (Levine & Kroemer, 2019). For example, Crohn's Disease is associated with ATG16L1, breast and ovarian cancer with BECN1, or diabetes and multiple sclerosis with CLEC16A (Levine & Kroemer, 2019). Previous studies have also shown that mutations in autophagy related genes can cause some neurodegenerative disorders, cancer, inflammatory disorders (Levine & Kroemer, 2019).

The *ATG13* gene is responsible for aiding in regulation of autophagy as well as many other functions. ATG13 is an accessory protein in the ULK1/2 complex, responsible for nutrient and energy signals in coordinating the induction of autophagy (Hieke et al., 2015). Other responsibilities of this gene include immune function, the stress response, and oncogenesis (Li et al., 2020). ATG13 is a target of the TOR kinase signaling pathway and is also seen to be essential for mitophagy (the removal of damaged mitochondria) and autophagosome formation (Stephan et al., 2009). TOR, or target of rapamycin, pathways respond to nutrient conditions by being conserved negative regulators of autophagy (Chang & Neufeld, 2009). When TOR becomes dysfunctional or stops working, this can have negative effects, activating a multiprotein complex containing ATG13 and further multiprotein complexes (Chang & Neufeld, 2009). In unfavourable growth conditions, this can cause a decrease in affinity for ATG1 since the multiprotein complex is regulated by the TOR signaling pathway which phosphorylates ATG13 (Chang & Neufeld, 2009). Overall, the *ATG13* gene plays a crucial role in the human body.

1.4 Purpose of study

The purpose of this study is to determine if *ATG13* gene dysfunction is present in diverse Canadian individuals with post-infectious syndromes. Having seen evidence of overexpression of this gene in Chronic Fatigue Syndrome (Gottschalk, et al., 2022), we hypothesize that ATG13 function will be altered in other post-infectious syndrome participants, predicting an over expression of this gene within the infected participants.

Methods

2.1 Human blood collection and sera collection

The blood collection and sera extraction were completed as described in Nelson, 2023. The blood collection was approved by Mount Allison Research Ethics Board (REB #: 103265/ 2014-028). At the time of blood collection, participants provided basic demographic information, extensive information on their potential exposure to ticks and tick-borne pathogens, an extensive list of symptoms consistent with tick-borne and other diseases, and information on any diagnoses, treatment, and response to treatment. As all the post-infectious conditions being evaluated in this work are clinically diagnosed with overlapping signs and symptoms, the specific diagnosis provided by the participants can reflect access to physicians; without access they might not have a diagnosis and which physicians provide which diagnosis may differ between countries, physician speciality and prior experience. Additionally, as is common for those with chronic illnesses without recourse to treatment able to alleviate symptoms, participants “wandered” between physicians, which resulted in multiple diagnoses in many cases. In order to assess ATG expression for each post-infectious syndrome, participants were included in each category for which they had that diagnosis. This means that any given participant could be represented once to four times. For Lyme disease, as is consistent with work in the field, participants were further categorized by those with diagnoses (diagnosed Lyme disease), probable Lyme disease for participants who reported onset of symptoms following either or both of a tick bite and EM rash or possible Lyme disease, for those reporting a tick bite or rash but with unclear disease trajectory. Participants with Lyme disease were further categorized by whether they had acute or chronic Lyme disease and their response to treatment: no treatment, treatment with no recovery, treatment with partial recovery and treatment with full recovery.

2.2 Enzyme-linked immunosorbent assay (ELISA)

The ELISA protocol was followed by MyBioSource Antibody Protein ELISA Kit protocol. To conduct the enzyme-linked immunosorbent assay (ELISA), three human ATG13 kits, each with a 96 well plate, were ordered from MyBioSource (Cat No.: MBS7615012, Lot No.: H6521I078, Lot No.: FN231012)). Each plate can test 44 samples, doing duplicates of each, including eight standard dilutions. This sandwich ELISA works by having the capture antibody coated on the plate, then the specific antigen is added to bind, then further primary and secondary antibodies are added to overall detect a quantifiable amount of the ATG13 protein. To begin, the concentration of the target protein in the test sample was estimated, and based off previous literature, a trial run was conducted prior to the rest of the samples. This trial run used healthy samples 1 and 2, doing duplicates of each with a sera concentration of 1:4 and 1:200 of each based on previous literature to determine the appropriate concentration for the rest of the samples. The concentration of 1:200 was used as values were consistent with using less sera sample. In all cases, reagents were mixed and brought to room temperature for 20 minutes before use.

A standard curve was created to ensure proper functioning of the ELISA kit and to determine the concentration of ATG13 in the samples. Standards were made by adding 1ml sample dilution buffer into a standard tube which was labeled as ‘zero tube’, acting as the undiluted sample, then kept at room temperature for 10 minutes, followed by a thorough mixing. Seven tubes were labeled with the corresponding dilutions: 1/2, 1/4, 1/8, 1/16, 1/32, 1/64, and blank. Next, 0.3ml of Sample Dilution Buffer was added into each of the tubes. 0.3ml was then added from the Standard solution (labeled zero tube), into the first tube (1/2). This tube was mixed thoroughly then 0.3ml was transferred from the first tube (1/2) to the second tube (1/4) and mixed thoroughly. 0.3ml was then transferred from the second tube to the third tube, then mixed, and continued until the sixth tube. For the blank control, Sample Dilution Buffer was used.

Next, the Biotin-labeled Antibody Working Solution was prepared within 1 hour before the experiment. The total volume of the working solution was calculated by using the following formula: 0.1ml/well x quantity of wells (allowing for .1-.2ml more than total volume). The Biotin-detection antibody was diluted at a 1:100 with the Antibody Dilution Buffer (Batch No.: MHC87-004, Batch No.: MHC87-003), then mixed thoroughly.

The HRP-Streptavidin Conjugate (SABC) Working Solution (Batch No.: S1000-009, Batch No.: S1000-005) was prepared about 30 minutes before the experiment. The total volume of the working solution was calculated by using the following formula: 0.1ml/well x quantity of wells (allowing for .1-.2ml more than total volume). The SABC antibody was diluted at a 1:100 with the SABC Dilution Buffer (Batch No.: HF2RP-004, Batch No.: HF2RP-003), then mixed thoroughly.

Prior to completing the assay procedure, TMB substrate was equilibrated at 37ºC for 30 minutes in the incubator (Fisher Scientific). Sample positions were recorded in a lab book to ensure correct positioning. Standards were prepared by aliquoting 100ul of solution from the tube labeled zero, 1/2, 1/4, 1/8, 1/16, 1/32, 1/64, and blank into the corresponding standard wells. Next, 100ul of diluted samples were added into test sample wells, with duplicates of each. The plate was then sealed and incubated for 90 minutes at 37ºC. After incubation, the cover was removed, and the plate contents were discarded by pipetting liquid out. The plate was washed two times with Wash Buffer by pipetting wash buffer into wells, allowing plate contents to soak in the buffer for 1-2 minutes each wash with gentle agitation, then removing the buffer by pipetting it out, then clapping the plate upside down on absorbent filter paper. 100ul of Biotin-labeled antibody working solution was then added into each well, then sealed and incubated for 60 minutes at 37ºC. After incubation, the cover was removed, and the plate contents were discarded by pipetting liquid out. The plate was washed three times with Wash Buffer by pipetting wash buffer into wells, allowing plate contents to soak in the buffer for 1-2 minutes each wash with gentle agitation, then removing the buffer by pipetting it out, and finally clapping the plate upside down on absorbent filter paper. 100ul of SABC-labeled working solution was then added into each well, then sealed and incubated for 30 minutes at 37ºC. After incubation, the cover was removed, and the plate contents were discarded. The plate was washed five times with Wash Buffer, clapping the plate on absorbent filter paper between washes and allowing to soak in the buffer for 1-2 minutes each wash. 90ul of TMB substrate was then added into each well, then sealed and incubated for 15 minutes at 37ºC. Once a colour change was observed from clear to blue, 50ul of stop solution (sulphuric acid solution) was added into each well, observing a colour change from blue to yellow. The plate was inserted into a Microplate Reader (AMR-100 Microplate Reader, Montreal Biotech Inc. Cat No.: MBIZLQ-900) at an absorbance of 450nm directly after the stop solution was added. Results were graphed using Microsoft Excel (version 16.66.1) and later graphed on RStudio (version 1.4.1717).

2.3 Immunohistochemistry

To begin immunohistochemistry, various solutions were needed to be mixed according to the following recipes:

10% goat serum in 1X PBS + 1% BSA:

$C_1V_1=C_2V_2$ $V_1= (10\%)(10mL)/100\% = 1mL$ 100% goat serum in 9mL 1X PBS + 1%BSA

1X PBS with 0.025% Triton X-100:

0.025mL of Triton X-100 into 100mL 1X PBS

1X PBS + 1% BSA:

$c=m/v$ $m=c*v$ $m=(1\%)(50mL)$ $m=0.1g$ 0.5g BSA into 50mL 1X PBS = 1% BSA

Primary antibody in 1% BSA and PBS

20uL primary antibody + 180uL BSA+PBS

Human brain slides were provided from the Mount Allison Lyme Disease BioBank (REB 2016-042/101796). One sample, from a brain known to be infected with *Borrelia burgdorferi,* was used as the positive biological control. Two samples from a brain previously known to have had a concussion were used, one as the negative biological control, to directly compare to a brain with post-infectious syndromes using the same secondary antibody as the positive biological control, and one as the negative technical control, with water instead of the secondary antibody to show that ATG13 is the only protein expressed.

The slides with tissue sections were dewaxed by baking at 60ºC in oven for 20 minutes. Slides were then immersed in serial 100% xylene baths for 5 minutes each. Next, slides immersed through serial immersion of 95% ethanol, 70% ethanol, 50% ethanol, distilled H2O, each for 5 minutes for powerful cleaning and rinsing.

For the immunohistochemistry procedure, slides were washed twice in 1X PBS (Lot #O7A62810) with 0.025% Triton X-100 (Lot #095K01221) with gentle agitation for 5 minutes. Then, slides were blocked in 10% goat serum (Lot #1007) with 1% BSA (Lot # SLBP1160V) in PBS at room temperature for 2 hours by pipetting drops of serum/BSA/PBS onto the slides to coat them. Slides were drained and gently wipes around the sections with tissue paper. Rabbit polyclonal to KIAA0652/ATG13 (ab105392) primary antibody was diluted using above calculations in 1% BSA in PBS was applied and slides were then incubated at 4ºC overnight. Slides were rinsed twice, five minutes each with gentle agitation using 1X PBS with 0.025% Triton X-100.

For detection, the secondary antibody, a goat to rabbit FITC-labelled antibody (ab7086, Lot #GR3254443-13), diluted with a concentration of 1:100 using 1% BSA and PBS was added to the slides and incubated at room temperature in the dark (to avoid photobleaching) for 1 hour. Slides were rinsed three times, five minutes each with 1X

PBS. 0.1% TrueBlack (Biotium, Lipofuscin Autofluorescence Quencher, Cat No. 23007) diluted in 70% ethanol was added and left for 20 minutes. Slides were washed twice, five minutes each with 1X PBS. DAPI (4',6-diamidino-2-phenylindole) was added to the slides which were then mounted with mounting medium. A cover slip was added to each slide and the edges of the coverslip were sealed with nail polish. Slides were then imaged using a Leica DM LS2 microscope (type 11 020 518 016), with ultraviolet LEP Ltd. arc lamp (Lot #990002). 40X and 100X magnification were used to image the specimens. Images were captured on an iPhone 11 camera.

2.4 ATG13 regulation by transcription factors

It is known that euchromatic histone methyltransferase 2 activates the Jak-Stat pathway, responsible for homeostasis and immune function. The Jak-Stat pathway is also known to regulate the AP-1 transcription factor. To determine if there was a connection between ATG13 and the AP-1 transcription factor, NIH Gen Bank was used to find the gene sequence of ATG13 in humans. The first 4921 nucleotides of the *ATG13* gene sequence were inputted into a transcription factor sequence binding site (ALGGEN – PROMO) to show transcription factor binding sites, including AP-1.

2.5 Statistical analysis

ELISA assay results produced a calorimetric response quantified by using a spectrophotometer. After absorbance values were recorded from the spectrophotometer, these values were first visualized using Microsoft Excel (version 16.66.1) and later graphed on RStudio (version 1.4.1717). Averages of each duplicate were calculated using Microsoft Excel. The following tests were all performed using RStudio. An ANOVA test was used to determine significant difference between all the groups. A Tukey honest significant difference test was used to compare the means of every post-infectious syndrome to every other post-infectious syndrome to show statistical difference between any of these groups.

2.6 Generative AI disclosure

I can confirm that I did not use generative AI to write this thesis. Citations were found from Google Scholar and PubMed, and generated using Zotero.

Results

3.1 ELISA results

People with chronic illnesses of presumed infectious origin were solicited for a study on infectious agents, in particular Lyme disease. The participants were categorized by post-infectious syndrome based on participant-provided information, as detailed in the Methods. The categories were: healthy, Chronic Fatigue Syndrome, fibromyalgia, multiple sclerosis, diagnosed Lyme, probably Lyme, and possible Lyme (Table 2-8).

To perform the ELISA testing for ATG13 in sera from these participants, first a standard dilution was performed to determine serum dilution that fell into the linear range (Table 1) (Figure 1). The chosen sera dilution factor was 1:200.

Table 1. Average absorbance values recorded from standard dilution.

Dilution	Average absorbance value
1	1.544
0.5	1.243
0.25	0.826
0.125	0.552
0.0625	0.708
0.0312	0.453
0.016	0.343
0	0.261

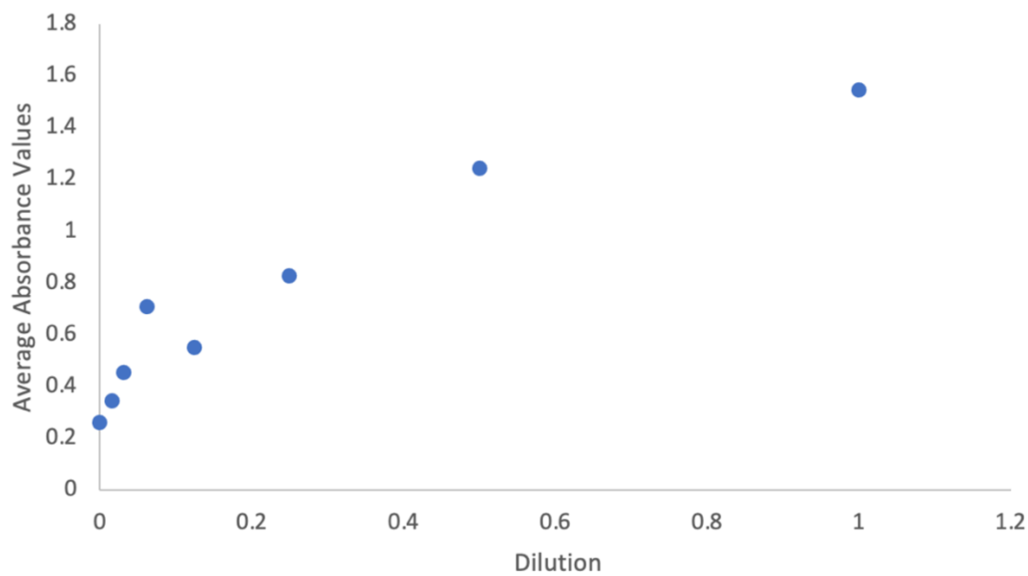

Figure 1. Graph of standard curve from standard dilution with corresponding average absorbance values.

Absorbance values were recorded for duplicates or quadruplicates of sample, and averages and standard error were calculated (Tables 2-8). The healthy control samples showed a fairly consistent ATG13 expression (Figure 2) with an average of 0.308308. These samples were set as zero when analyzing the post-infection samples by subtracting the average absorbance values for healthy participant samples from each of the post-infectious syndrome participant samples. The resulting value of post-infectious syndrome participant absorbance values were graphed to show over or under expression of the post-infectious syndromes (Figures 2-8).

Table 2: Participant sample ID, diagnosis, duplicate 1 and 2 absorbance values, calculated average absorbance values, and calculated standard error values for healthy participants.

DA ID	Diagnosis	Absorbance value (duplicate 1)	Absorbance value (duplicate 2)	Absorbance value (average)	Standard error
DA-01	Healthy	0.292	0.467	0.3795	0.0875
DA-02	Healthy	0.130	0.374	0.252	0.122
DA-05	Healthy	0.178	0.279	0.2285	0.0505
DA-10	Healthy	0.443	0.383	0.413	0.03
DA-11	Healthy	0.217	0.166	0.1915	0.0255
DA-13	Healthy	0.413	0.386	0.3995	0.0135
DA-20	Healthy	0.345	0.385	0.365	0.02
DA-27	Healthy	0.281	0.229	0.255	0.026
DA-35	Healthy	0.457	0.333	0.395	0.062
DA-36	Healthy	0.226	0.116	0.171	0.055
DA-104	Healthy	0.511	0.253	0.382	0.129
DA-109	Healthy	0.438	0.302	0.370	0.068
DA-131	Healthy	0.252	0.225	0.2385	0.0135

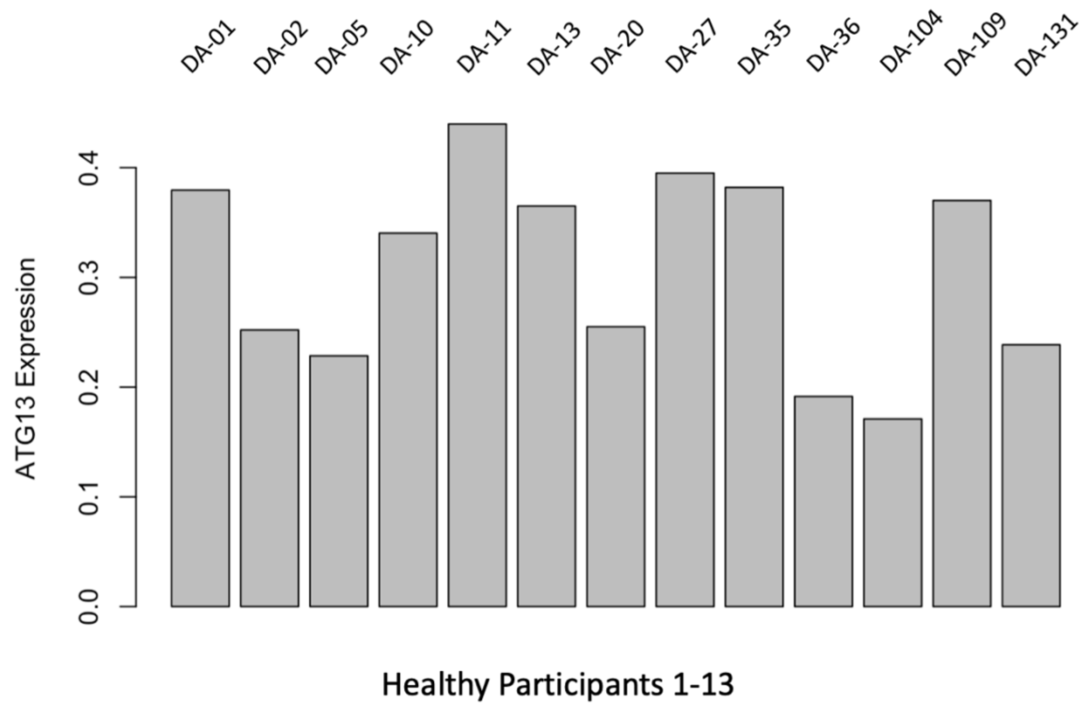

Figure 2. ATG13 expression for healthy participants 1-13.

Table 3: Participant sample ID, diagnosis, duplicate 1 and 2 absorbance values, calculated average absorbance values, and calculated standard error values for healthy participants. Participants may have more than one diagnosis: Lyme (L), multiple sclerosis (MS), Chronic Fatigue Syndrome (CF), fibromyalgia (F), probable Lyme (probL), and possible Lyme (possL).

DA ID	Diagnosis	Absorbance value (duplicate 1)	Absorbance value (duplicate 2)	Absorbance value (average)	Standard error
DA-19	CF, F, L	0.324	0.212	0.268	0.056
DA-23	MS, CF, F, L	0.3555	0.2575	0.3065	0.049
DA-26	CF, F, L	0.2715	0.3075	0.2895	0.018
DA-32	CF, L	0.2345	0.485	0.35975	0.12525
DA-37	CF, F	0.255	0.235	0.245	0.01
DA-44	MS, CF, F, L	0.318	0.222	0.27	0.048
DA-63	CF, F, L	0.433	0.402	0.4175	0.0155
DA-80	L, CF, F	0.184	0.242	0.213	0.029
DA-94	CF, L	0.313	0.197	0.255	0.058
DA-142	CF, F	0.347	0.345	0.346	0.001
DA-155	CF, F, probL	0.584	0.443	0.5135	0.0705
DA-158	L, CF, F	0.402	0.406	0.404	0.002

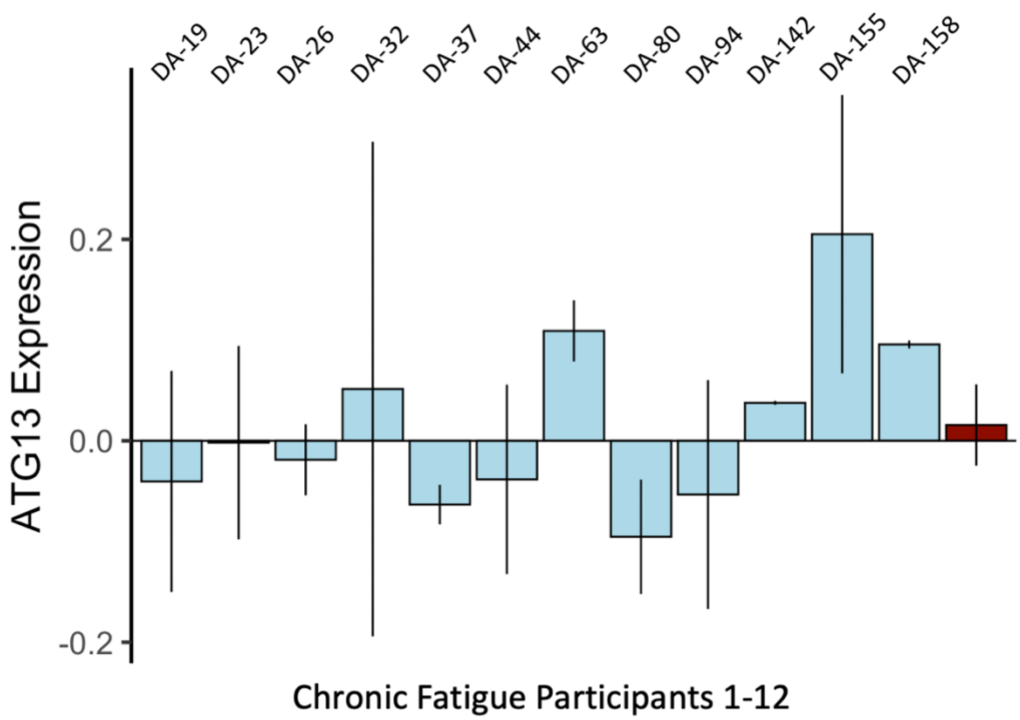

Figure 3. *ATG13* gene expression for Chronic Fatigue Syndrome participants 1-12. The overall average expression is shown in dark red on the far right of the graph. 95% confidence intervals are presented as the vertical lines. No significant pattern of ATG13 expression was determined (p=1.000000).

Table 4: Participant sample ID, diagnosis, duplicate 1 and 2 absorbance values, calculated average absorbance values, and calculated standard error values for fibromyalgia participants. Participants may have more than one diagnosis: Lyme (L), multiple sclerosis (MS), Chronic Fatigue Syndrome (CF), fibromyalgia (F), probable Lyme (probL), and possible Lyme (possL).

DA ID	Diagnosis	Absorbance value (duplicate 1)	Absorbance value (duplicate 2)	Absorbance value (average)	Standard error
DA-03	F	0.338	0.359	0.3485	0.013
DA-04	F	0.309	0.335	0.322	0.0115
DA-16	F, probL	0.348	0.325	0.3365	0.056
DA-19	F, CF, L	0.324	0.212	0.268	0.02075
DA-21	F, possL	0.343	0.3015	0.32225	0.049
DA-23	MS, CF, F, L	0.3555	0.2575	0.3065	0.03475
DA-25	MS, F, L	0.33	0.2605	0.29525	0.018
DA-26	CF, F, L	0.2715	0.3075	0.2895	0.013
DA-38	F, L	0.089	0.115	0.102	0.01
DA-37	CF, F	0.255	0.235	0.245	0.048
DA-44	MS, CF, F, L	0.318	0.222	0.27	0.0155
DA-63	CF, F, L	0.433	0.402	0.4175	0.0225
DA-70	F	0.241	0.286	0.2635	0.029
DA-80	L, CF, F	0.184	0.242	0.213	0.0805
DA-84	F	0.415	0.254	0.3345	0.02
DA-108	F, possL	0.574	0.534	0.554	0.0155
DA-120	F, probL	0.32	0.289	0.3045	0.0305
DA-141	F	0.262	0.323	0.2925	0.001
DA-142	CF, F	0.347	0.345	0.346	0.0705
DA-155	CF, F, probL	0.584	0.443	0.5135	0.002
DA-158	L, CF, F	0.402	0.406	0.404	0.013

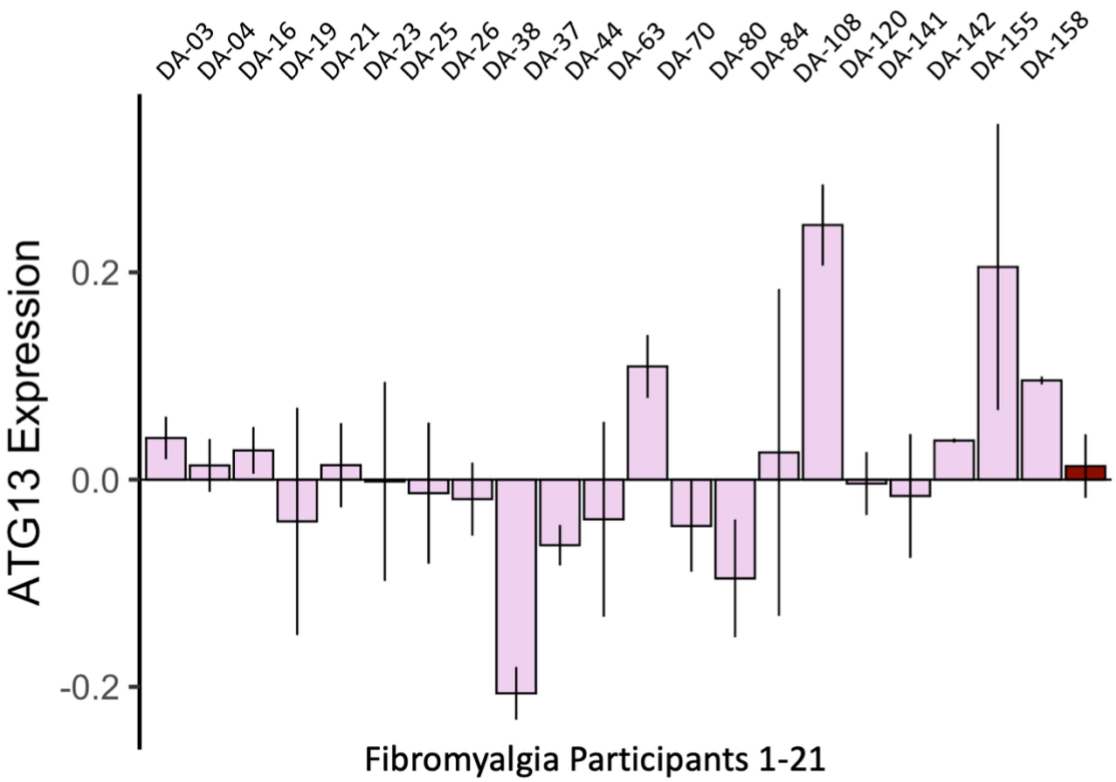

Figure 4. *ATG13* gene expression for fibromyalgia participants 1-21. The overall average expression is shown in dark red on the far right of the graph. 95% confidence intervals are presented as the vertical lines. No significant pattern of ATG13 expression was determined (p=0.99992754).

Table 5: Participant sample ID, diagnosis, duplicate 1 and 2 absorbance values, calculated average absorbance values, and calculated standard error values for multiple sclerosis participants. Participants may have more than one diagnosis: Lyme (L), multiple sclerosis (MS), Chronic Fatigue Syndrome (CF), fibromyalgia (F), probable Lyme (probL), and possible Lyme (possL).

DA ID	Diagnosis	Absorbance value (duplicate 1)	Absorbance value (duplicate 2)	Absorbance value (average)	Standard error
DA-22	MS, L	0.3005	0.196	0.24825	0.05225
DA-23	MS, CF, F, L	0.3555	0.2575	0.3065	0.049
DA-25	MS, F, L	0.33	0.2605	0.29525	0.03475
DA-26	MS, F, L	0.2715	0.3075	0.2895	0.018
DA-40	MS, possL	0.242	0.262	0.252	0.01
DA-44	MS, CF, F, L	0.318	0.222	0.27	0.048
DA-48	MS	0.147	0.174	0.1605	0.0135
DA-64	MS, probL	0.209	0.139	0.174	0.035
DA-56	L, MS	0.2545	0.2325	0.2435	0.011
MS-81	MS	0.318	0.222	0.27	0.0155
MS-82	MS	0.433	0.402	0.4175	0.0225
MS-83	MS	0.241	0.286	0.2635	0.029
MS-84	MS	0.184	0.242	0.213	0.0805
MS-85	MS	0.415	0.254	0.3345	0.02
MS-86	MS	0.574	0.534	0.554	0.0155
MS-87	MS	0.32	0.289	0.3045	0.0305
MS-88	MS	0.262	0.323	0.2925	0.001
MS-89	MS	0.347	0.345	0.346	0.0705
MS-90	MS	0.584	0.443	0.5135	0.002
MS-157	MS	0.402	0.406	0.404	0.013

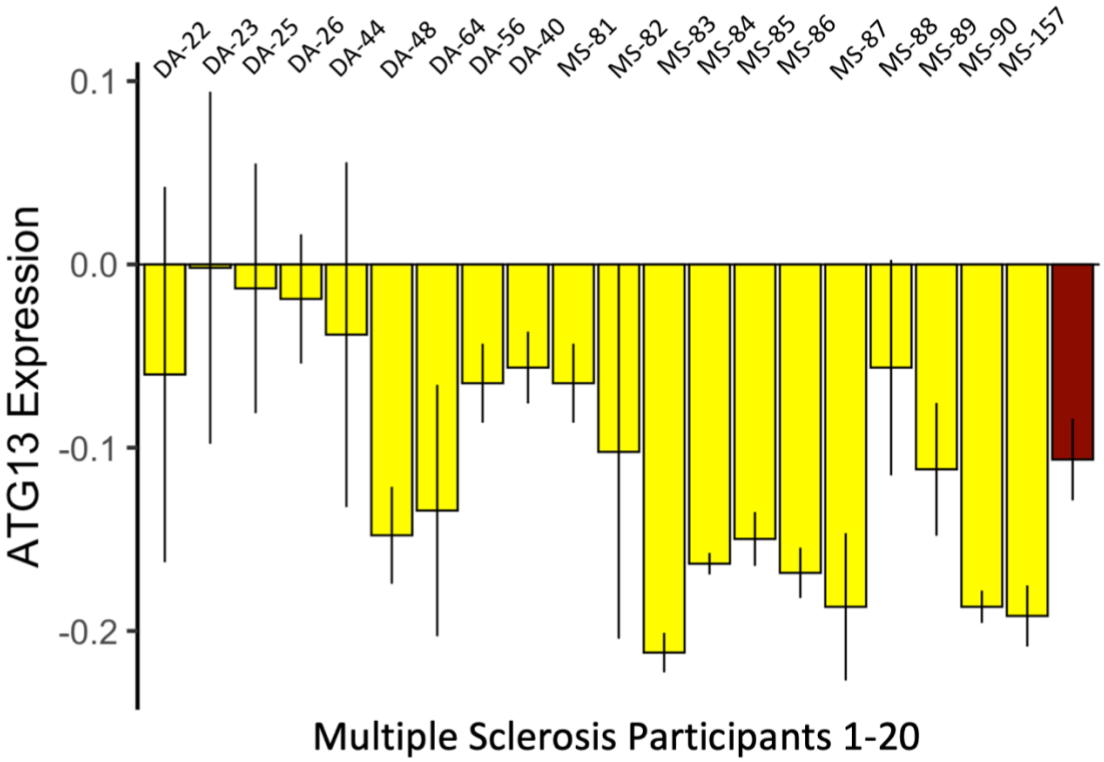

Figure 5. *ATG13* gene expression for multiple sclerosis participants 1-20. The overall average expression is shown in dark red on the far right of the graph. 95% confidence intervals are presented as the vertical lines. Significant under expression of ATG13 was determined (p=0.0192026).

Table 6: Participant sample ID, diagnosis, duplicate 1 and 2 absorbance values, calculated average absorbance values, and calculated standard error values for diagnosed Lyme participants. Participants may have more than one diagnosis: Lyme (L), multiple sclerosis (MS), Chronic Fatigue Syndrome (CF), fibromyalgia (F), probable Lyme (probL), and possible Lyme (possL).

DA ID	Diagnosis	Absorbance value (duplicate 1)	Absorbance value (duplicate 2)	Absorbance value (average)	Standard error
DA-12	L	0.2275	0.2085	0.218	0.0095
DA-18	L	0.3655	0.303	0.33425	0.0095
DA-19	L, CF, F	0.324	0.212	0.268	0.056
DA-22	L, MS	0.210	0.156	0.183	0.027
DA-23	MS, CF, F, L	0.3555	0.2575	0.3065	0.049
DA-25	MS, F, L	0.330	0.2605	0.29525	0.03475
DA-26	CF, F, L	0.2715	0.3075	0.2895	0.018
DA-32	CF, L	0.2345	0.485	0.35975	0.12525
DA-38	F, L	0.089	0.115	0.102	0.013
DA-44	MS, CF, F, L	0.318	0.222	0.27	0.048
DA-51	L	0.346	0.188	0.267	0.079
DA-56	MS, L	0.2545	0.2325	0.2435	0.011
DA-59	L	0.188	0.215	0.2015	0.0135
DA-62	L	0.197	0.1665	0.18175	0.01525
DA-63	CF, F, L	0.433	0.402	0.4175	0.0155
DA-75	L	0.099	0.162	0.1305	0.0315
DA-80	L, CF, F	0.184	0.242	0.213	0.029
DA-94	CF, L	0.313	0.197	0.255	0.058
DA-110	L	0.371	0.326	0.3485	0.0225
DA-137	L	0.426	0.318	0.372	0.054
DA-158	L, CF, F	0.402	0.406	0.1605	0.002

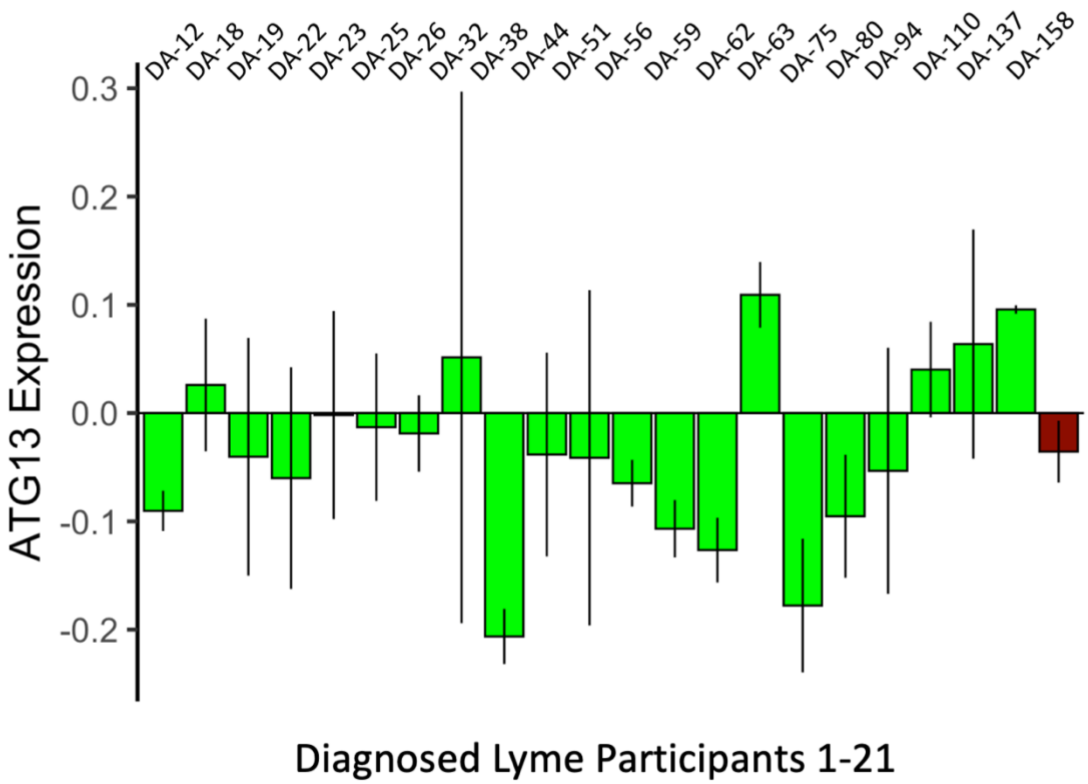

Figure 6. *ATG13* gene expression for diagnosed Lyme participants 1-21. The overall average expression is shown in dark red on the far right of the graph. 95% confidence intervals are presented as the vertical lines. No significant pattern of ATG13 expression was determined (p=0.9057558).

Table 7: Participant sample ID, diagnosis, duplicate 1 and 2 absorbance values, calculated average absorbance values, and calculated standard error values for probably Lyme participants. Participants may have more than one diagnosis: Lyme (L), multiple sclerosis (MS), Chronic Fatigue Syndrome (CF), fibromyalgia (F), probable Lyme (probL), and possible Lyme (possL).

DA ID	Diagnosis	Absorbance value (duplicate 1)	Absorbance value (duplicate 2)	Absorbance value (average)	Standard error
DA-06	probL	0.237	0.212	0.2245	0.0125
DA-16	F, probL	0.348	0.325	0.3365	0.0115
DA-64	MS, probL	0.209	0.139	0.174	0.035
DA-120	F, probL	0.32	0.289	0.3045	0.0155
DA-155	CF, F, probL	0.584	0.443	0.5135	0.0705

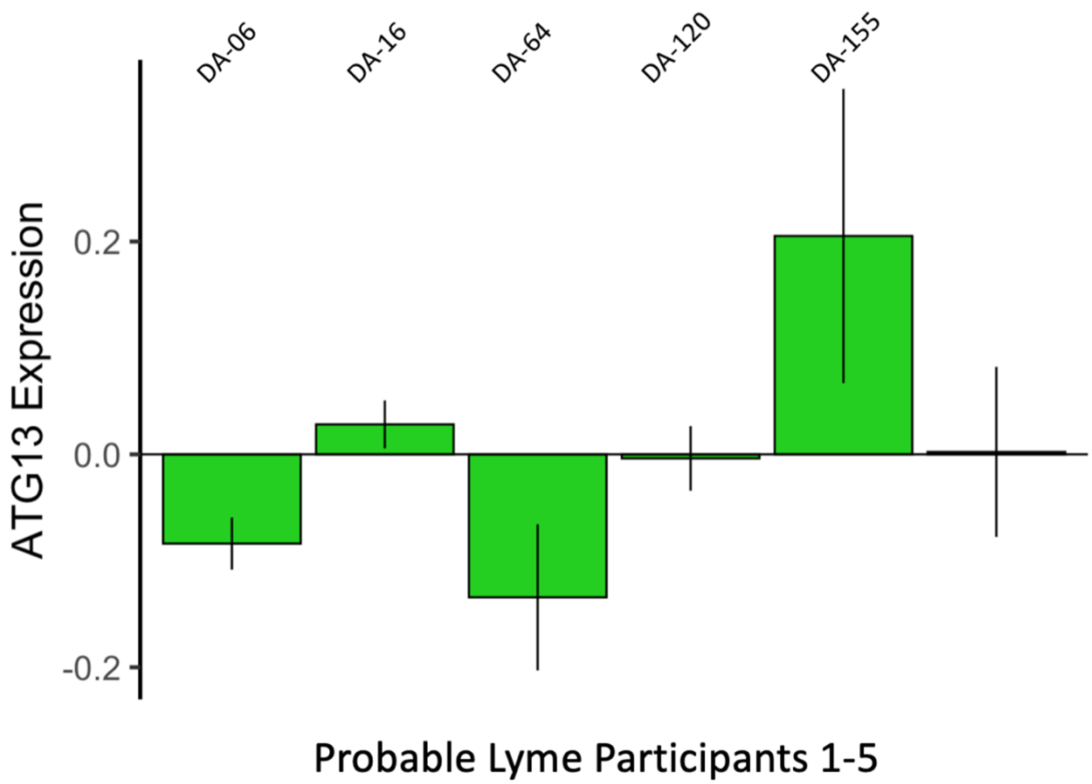

Figure 7. *ATG13* gene expression for probable Lyme participants 1-5. The overall average expression is shown in dark red on the far right of the graph. 95% confidence intervals are presented as the vertical lines. No significant pattern of ATG13 expression was determined (p=1.000000).

Table 8: Participant sample ID, diagnosis, duplicate 1 and 2 absorbance values, calculated average absorbance values, and calculated standard error values for possible Lyme participants. Participants may have more than one diagnosis: Lyme (L), multiple sclerosis (MS), Chronic Fatigue Syndrome (CF), fibromyalgia (F), probable Lyme (probL), and possible Lyme (possL).

DA ID	Diagnosis	Absorbance value (duplicate 1)	Absorbance value (duplicate 2)	Absorbance value (average)	Standard error
DA-21	F, possL	0.343	0.3015	0.32225	0.02075
DA-40	MS, possL	0.242	0.262	0.252	0.01
DA-108	F, possL	0.574	0.534	0.554	0.02

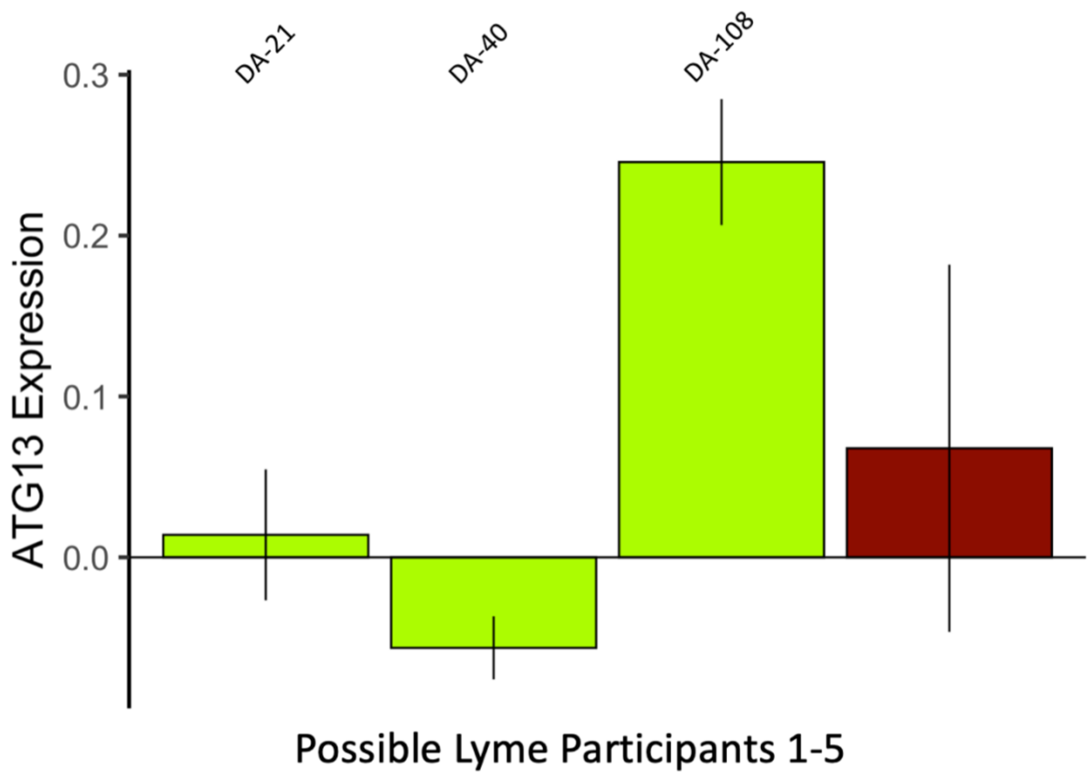

Figure 8. *ATG13* gene expression for possible Lyme participants 1-3. The overall average expression is shown in dark red on the far right of the graph. 95% confidence intervals are presented as the vertical lines. No significant pattern of ATG13 expression was determined (p=0.2587804).

To determine any statistically significant differences between the means of different groups, an ANOVA was conducted (p=2e-05) (Table 9). A Tukey test was run to determine the significant difference between each specific group. When comparing to healthy participants, this test showed a significant difference between multiple sclerosis participants and healthy participants (p=0.0192026) (Table 10).

Table 9. ANOVA summary of results for healthy, diagnosed Lyme, probable Lyme, possible Lyme, multiple sclerosis, fibromyalgia, and Chronic Fatigue Syndrome participants.

	Df	Sum Sq	Mean Sq	F value	Pr (>F)
Stacked groups	6	0.3286	0.05477	5.805	2e-05
Residuals	140	1.3209	0.00943		

Table 10. Results from Tukey test for healthy, diagnosed Lyme (lyme), probable Lyme (probL), possible Lyme (possL), multiple sclerosis (ms), fibromyalgia (f), and Chronic Fatigue Syndrome (cf) participants. Difference, lower limit, upper limit, and p adjacent value shown. Significant data represented under p adjacent values.

	diff	lwr	upr	P adj
lyme-healthy	-0.034940476	-0.12461810	0.054737147	0.9057558
probl-healthy	-0.001095238	-0.09077286	0.088582385	1.0000000
possl-healthy	0.068488095	-0.02118953	0.158165718	0.2587804
ms-healthy	-0.099547619	-0.18922524	-0.009869996	0.0192026
f-healthy	0.013761905	-0.07591572	0.103439528	0.9992754
cf-healthy	0.002500000	-0.08717762	0.092177623	1.0000000
probl-lyme	0.033845238	-0.05583238	0.123522861	0.9181162
possl-lyme	0.103428571	0.01375095	0.193106194	0.0127978
ms-lyme	-0.064607143	-0.15428477	0.025070480	0.3267274
f-lyme	0.048702381	-0.04097524	0.138380004	0.6666428
cf-lyme	0.037440476	-0.05223715	0.127118099	0.8734469
possl-probl	0.069583333	-0.02009429	0.159260956	0.2413261
ms-probl	-0.098452381	-0.18813000	-0.008774758	0.0214697
f-probl	0.014857143	-0.07482048	0.104534766	0.9988788
cf-probl	0.003595238	-0.08608238	0.093272861	0.9999997
ms-possl	-0.168035714	-0.25771334	-0.078358092	0.0000022
f-possl	-0.054726190	-0.14440381	0.034951432	0.5331287
cf-possl	-0.065988095	-0.15566572	0.023689528	0.3014926
f-ms	0.113309524	0.02363190	0.202987147	0.0042496
cf-ms	0.102047619	0.01237000	0.191725242	0.0148127
cf-f	-0.011261905	-0.10093953	0.078415718	0.9997721

3.2 Treatment and recovery results

Treatment and recovery status were observed to see if these factors had an impact on diagnosed Lyme, probable Lyme, and possible Lyme participants (Table 11).

Table 11. Participant sample ID, diagnosis, treatment status, and recovery status. Absorbance values found in tables 2-8. Participants may have more than one diagnosis: Lyme (L), multiple sclerosis (MS), Chronic Fatigue Syndrome (CF), fibromyalgia (F), probable Lyme (probL), and possible Lyme (possL).

DA ID	Diagnosis	Treatment status	Recovery status
DA-12	L	Treated	No recovery
DA-32	CF, L	Treated	No recovery
DA-40	MS, possL	Treated	No recovery
DA-137	L	Treated	No recovery
DA-158	L, CF, F	Treated	No recovery
DA-18	L	Treated	Partial recovery
DA-19	CF, F, L	Treated	Partial recovery
DA-22	MS, L	Treated	Partial recovery
DA-23	MS, CF, F, L	Treated	Partial recovery
DA-25	MS, F, L	Treated	Partial recovery
DA-26	CF, F, L	Treated	Partial recovery
DA-44	MS, CF, F, L	Treated	Partial recovery
DA-51	L	Treated	Partial recovery
DA-59	L	Treated	Partial recovery
DA-63	CF, F, L	Treated	Partial recovery
DA-94	CF, L	Treated	Partial recovery
DA-110	L	Treated	Partial recovery
DA-155	CF, F, L	Treated	Partial recovery
DA-38	F, L	Treated	Full recovery
DA-56	L, MS	Treated	Full recovery
DA-62	L	Treated	Full recovery
DA-6	MS, probL	Untreated	N/A
DA-16	F, probL	Untreated	N/A
DA-21	F, possL	Untreated	N/A
DA-64	MS, probL	Untreated	N/A
DA-75	L	Untreated	N/A
DA-80	L, CF, F	Untreated	N/A
DA-108	F, possL	Untreated	N/A
DA-120	F, probL	Untreated	N/A

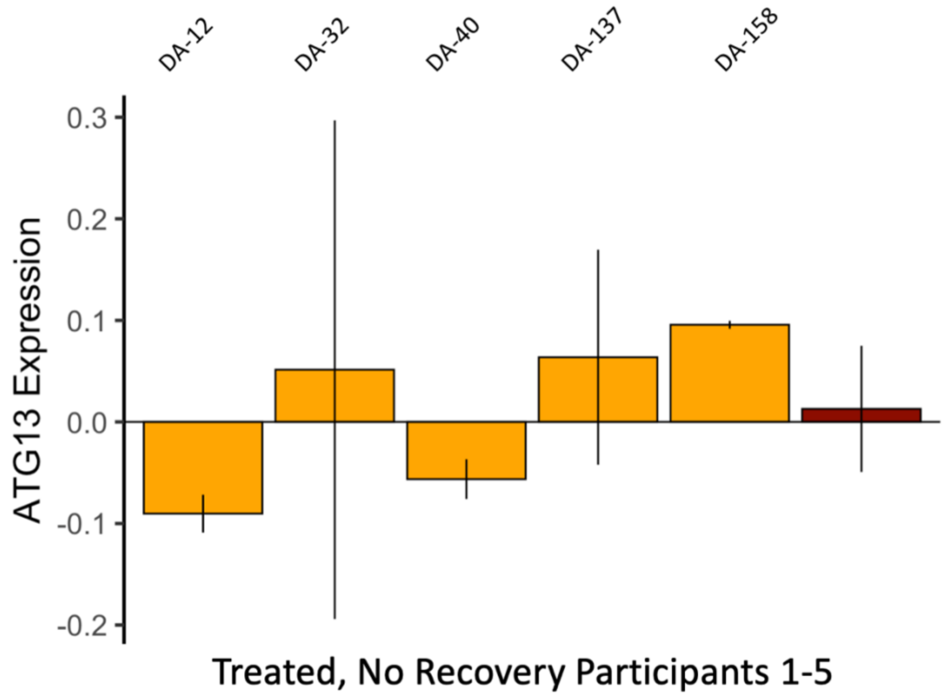

Figure 9. *ATG13* gene expression for treated, no recovery participants 1-5. The overall average expression is shown in dark red on the far right of the graph. 95% confidence intervals are presented as the vertical lines. No significant pattern of ATG13 expression was determined (p=0.9999924).

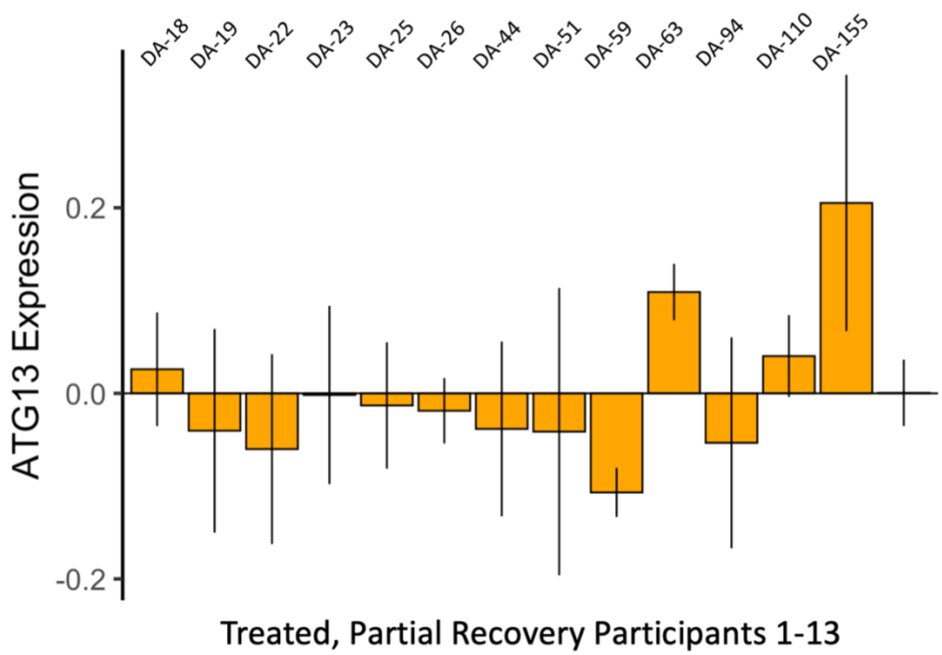

Figure 10. *ATG13* gene expression for treated, partial recovery participants 1-13. The overall average expression is shown in dark red on the far right of the graph. 95% confidence intervals are presented as the vertical lines. No significant pattern of ATG13 expression was determined (p=1.000000).

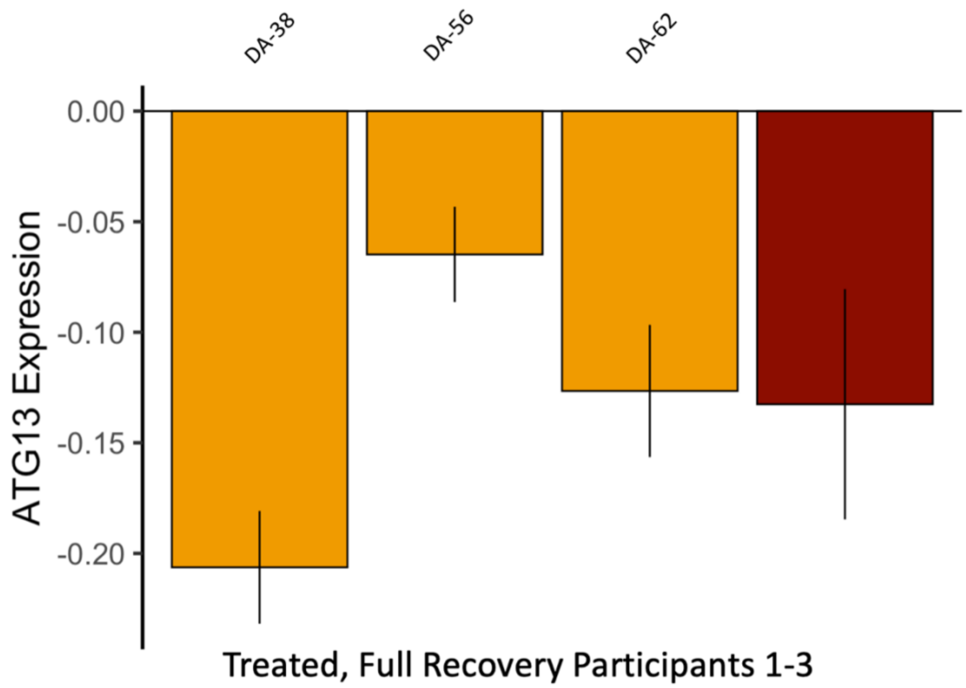

Figure 11. *ATG13* gene expression for treated, full recovery participants 1-3. The overall average expression is shown in dark red on the far right of the graph. 95% confidence intervals are presented as the vertical lines. Significant under expression of ATG13 was determined (p=0012155).

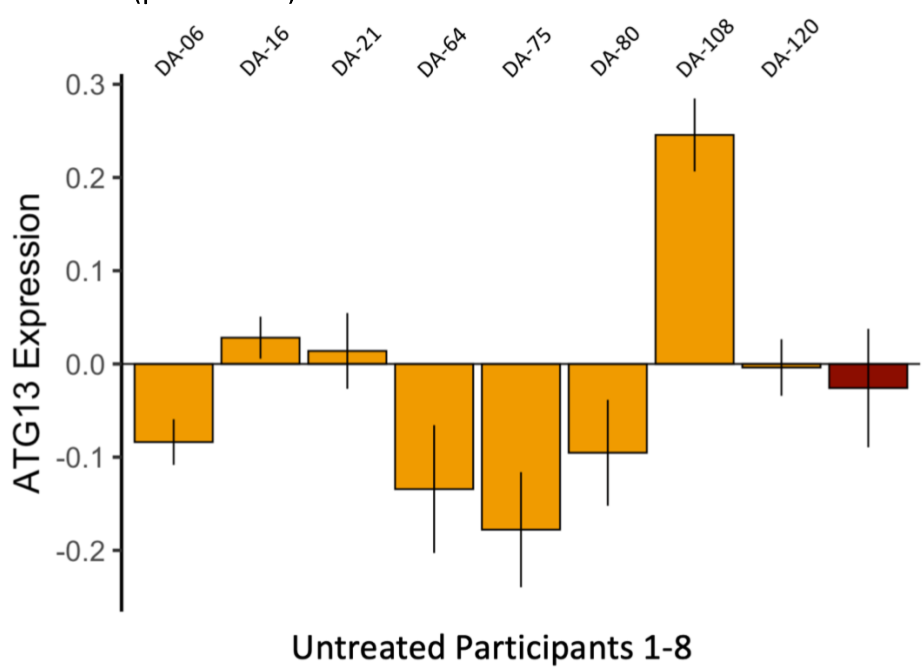

Figure 12. *ATG13* gene expression for untreated participants 1-8. The overall average expression is shown in dark red on the far right of the graph. 95% confidence intervals are presented as the vertical lines. No significant pattern of ATG13 expression was determined (p=0.7072948).

To determine any statistically significant difference between groups, an ANOVA was conducted (p=0.00024) (Table 12). A Tukey test was run to determine the significant difference between each specific group. When comparing to healthy participants, this test showed a significant difference between treated, fully recovered Lyme participants and healthy participants (p=0.0012155) (Table 13).

Table 12. ANOVA summary of results for healthy, treated no recovery, treated partial recovery, treated full recovery and untreated participants.

	Df	Sum Sq	Mean Sq	F value	Pr (>F)
Stacked groups	4	0.1900	0.04751	6.381	0.00024
Residuals	60	0.4467	0.00745		

Table 13. Results from Tukey test for healthy, treated no recovery (tnr), treated partial recovery (tpr), treated full recovery (tfr), and untreated (ut) participants. Difference, lower limit, upper limit, and p adjacent value shown. Significant data represented under p adjacent values.

	diff	lwr	upr	P adj
tnr-healthy	0.0025576923	-0.092626546	0.09774193	0.9999924
tpr-healthy	0.0005192308	-0.094665007	0.09570347	1.0000000
tfr-healthy	-0.1382307692	-0.233415007	-0.04304653	0.0012155
ut-healthy	-0.0431538462	-0.138338084	0.05203039	0.7072948
tpr-tnr	-0.0020384615	-0.097222700	0.09314578	0.9999969
tfr-tnr	-0.1407884615	-0.235972700	-0.04560422	0.0009470
ut-tnr	-0.0457115385	-0.140895777	0.04947270	0.6610004
tfr-tpr	-0.1387500000	-0.233934238	-0.04356576	0.0011557
ut-tpr	-0.0436730769	-0.138857315	0.05151116	0.6980330
ut-tfr	0.0950769231	-0.000107315	0.19026116	0.0503952

3.3 Immunohistochemistry results

To further explore the results found from the ELISA data, immunohistochemistry was completed to visualize ATG13 protein in brain slices. Two slides from a deceased human participant with a concussion were used, the first as a negative biological control (A-5-2) and the second as a negative technical control (A-7-2). A third slice from a deceased human participant with *Borrelia burgdorferi* infection was used as the positive sample (A16) (Table 14). The specimen from the concussion individual treated with primary antibody showed minimal fluorescence. There were a few fluorescent spots, but most fluorescence was dust on the slides as the spots were larger than expected (Figure 13). The specimen from the concussion individual treated without primary antibody showed no fluorescence (Figure 14). Sample BB3 showed abundant fluorescence of the correct size and shape compared to literature (Figure 15). This shows a difference in the intracellular location and distribution of the ATG13 protein in one individual with a post-infectious syndrome compared to participants without.

Table 14. Sample information for three brain slices showing the sample ID, slice ID, if the sample was treated with primary antibody, and if there was fluorescence from staining visible.

	Sample ID	Slice ID	Treated with primary antibody	Fluorescence of ATG13 visible
Negative biological control	A16-33	A-5-2	Yes	Minimal
Negative technical control	A16-33	A-7-2	No	None
Positive sample	BB3	A16	Yes	Abundant

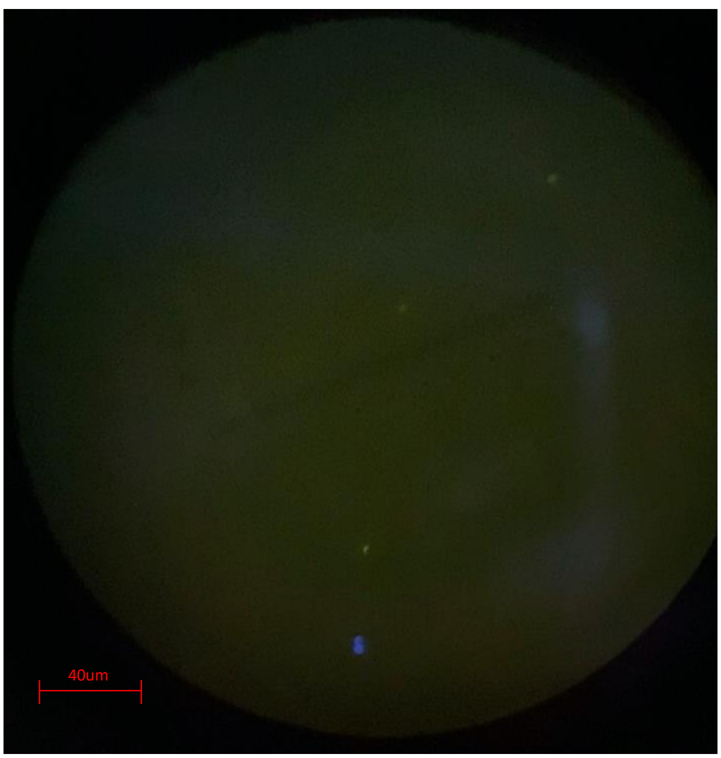

Figure 13. Slice A-5-2 negative biological control under 1000X total magnification with fluorescent lighting showing minimal fluorescence.

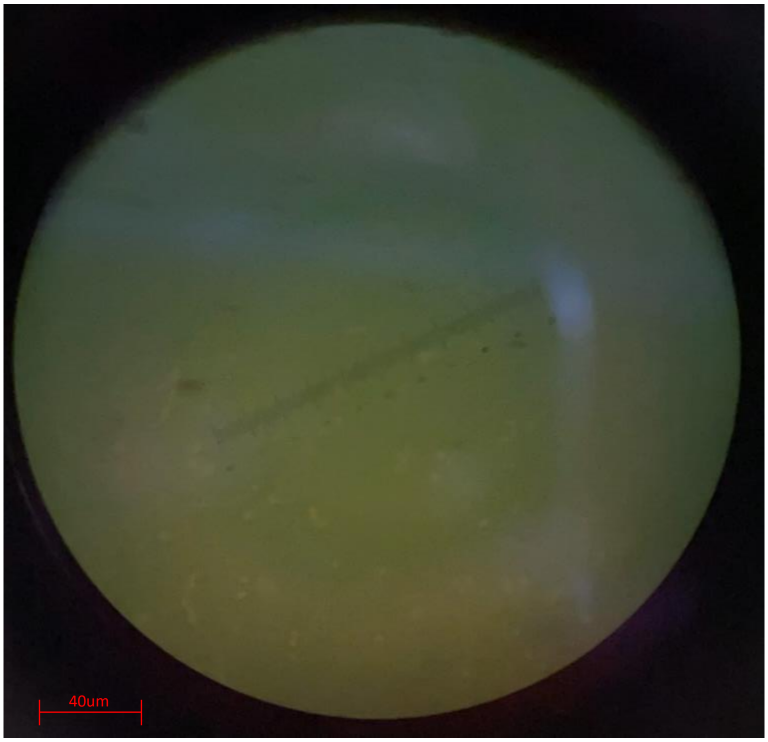

Figure 14. Slice A-7-2 negative technical control under 1000X total magnification with fluorescent lighting showing no fluorescence.

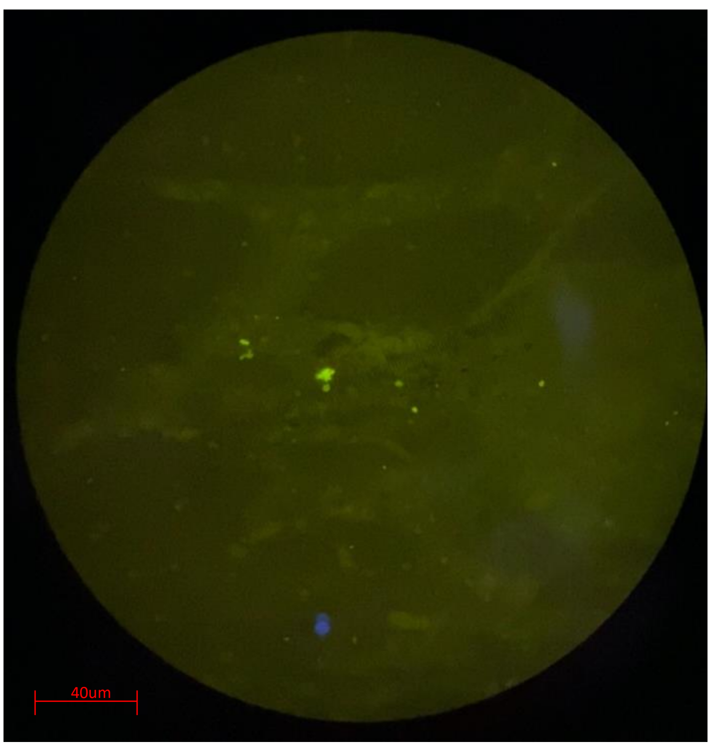

Figure 15. Slice A16 positive sample under 1000X total magnification with fluorescent lighting showing abundant fluorescence.

3.4 ATG13 regulation by transcription factors

To examine *ATG13* gene regulation, the first 4921 nucleotides in the gene sequence were scanned for transcription factor binding sites using the online transcription factor binding site tool, ALGGEN – PROMO, to look for binding sites for the AP-1 transcription factor. AP-1 can be activated by the Jak-Stat pathway – a pathway responsible for cell maintenance, hematopoiesis, and the inflammatory response, so this transcription factor was further investigated for ATG13. Eleven AP-1 transcription factor binding sites were found clustered in the 3000-4000bp area, suggesting it could be a potential regulator of ATG13 (Table 15).

Table 15. Nucleotide number where transcription factor AP-1 was found within the gene sequence from ATG13 in humans.

Transcription factor	Nucleotide number
AP-1	1371
	1379
	3055
	3063
	3235
	3243
	3397
	3405
	3590
	3655
	3663
	3881
	3889

Discussion

The goal of this study was to investigate *ATG13* gene expression in presumed post-infectious syndromes, Chronic Fatigue Syndrome, multiple sclerosis, fibromyalgia, diagnosed Lyme, probable Lyme, and possible Lyme.

4.1 Lyme disease

The Lyme samples (diagnosed, probable, and possible) often showed under-expression of ATG13 relative to the healthy controls, but it was not statistically significant. When comparing ATG13 expression from participants who were untreated, or treated with partially, or unresolved illness, there was again no significant difference. For the treated and fully recovered participants, however, there was a significant under expression of ATG13. This demonstrates that antibiotic treatment may influence ATG13 expression. If the treated but non-responsive samples were eliminated as probably incorrectly diagnosed participants, there was still not a statistical difference.

4.2 Chronic Fatigue Syndrome

Results of *ATG13* gene expression for Chronic Fatigue Syndrome samples showed no significant pattern of ATG13 expression. The study by Gottschalk and colleagues (2022) looked at Chronic Fatigue Syndrome participants and found an elevated level of ATG13 (Gottschalk et al., 2022). The results of this study differ from the results found by Gottschalk and colleagues (2022) as there was no clear pattern of ATG13 expression for samples from people with Chronic Fatigue Syndrome. This may be because the participants in the Gottschalk study were carefully selected, age and sex matched and from one clinic, while the participants in this study represent a more real-world sample population.

4.3 Fibromyalgia

Results of *ATG13* gene expression for fibromyalgia samples showed no significant pattern of ATG13 expression. This suggests that alteration function of ATG13 does not occur in people with fibromyalgia.

4.4 Multiple sclerosis

Results of *ATG13* gene expression for multiple sclerosis showed significant under expression. Antibiotics are not a common treatment for multiple sclerosis (Hauser & Cree, 2020), meaning that this is likely not the cause for the under expression of ATG13. Multiple sclerosis is a complex, multifactorial disease with genetic and environmental influences (Bjørnevik et al., 2023). It is postulated that infectious agents are a key environmental factor, with Epstein-Barr virus as the current prime candidate (Bjørnevik et al., 2023).

4.5 Immunohistochemistry

For the results of immunohistochemistry, there was a visual difference in expression of ATG13 in the brain slice from a person infected with *Borrelia burgdorferi* compared to a brain slice from a person with a concussion. The brain slice from the person infected with *Borrelia burgdorferi* showed ATG13 protein fluorescing, while there was no or minimal fluorescence in the brain slides from a person with a concussion. This suggests that *ATG13* gene acts differently in people with post-infectious syndromes compared to people without post-infectious syndromes. More samples are needed to determine if this is significant as only one brain slide per treatment was conducted and there could be changes due to difference in age or sex.

4.6 ATG13 regulation by transcription factors

The transcription factor, AP-1, may regulate ATG13 based on the presence of a cluster of AP-1 binding sites in the 5’ region of the *ATG13* gene sequence. A previous study from 2015 demonstrated that the histone H3 lysine 9 methyltransferase *G9a* is responsible for activating the Jak-Stat pathway (Merkling et al., 2015). The Jak-Stat pathway is crucial for many homeostatic and developmental processes such as stem cell maintenance, organismal growth, hematopoiesis, and immune cell development (Harrison, 2012). The Jak Stat pathway was then shown to activate the transcription factor, AP-1 (Merkling et al., 2015). Now, with the results found in this present study, it appears that AP-1 controls ATG13, suggesting that AP-1 may function differently in people with post-infectious syndromes. Exposure to epigenetic factors such as viruses or bacteria may cause this signaling cascade to function differently, resulting in the differences in *ATG13* gene expression, but this is yet to be tested.

4.7 Comparison to other studies

Although there has been little further research on the connection of ATG13 and post-infectious syndromes, recent studies have looked at other activities of ATG13 in the cell. A recent study looked at microRNA (bta-miR-2904) and how it targets ATG13, overall resulting in the inhibition of bovine viral diarrhea virus replication (Yang et al., 2022). The study explains how new research is showing an interaction between viruses and autophagy, specifically ATG13, and the regulation of autophagy may be used to potentially treat or prevent diseases that are caused by critical viral pathogens (Yang et al., 2022). Another study found that ATG13 is involved in the immune response during pathogen invasion in blood clams (Wu et al., 2023). This study investigated the poorly understood role of ATG13 in invertebrates, finding that ATG13 plays a role in more than just mammals (Wu et al., 2023). With ATG13 functioning in both vertebrates and invertebrates, this could suggest it's essential function in immunity and autophagy. A review from 2023 provides insight on the not yet fully explained relationship between autophagy and SARS-CoV-2, providing a rationale for a future study investigating *ATG13* gene expression in people experiencing long covid.

4.8 Limitations

There are limitations to this study, starting with a limited sample size, both of sera and brain samples; both were limited by availability in the biobank. For Lyme disease, multiple sclerosis, chronic fatigue, and fibromyalgia, all are clinical diagnoses, poorly supported by objective tests so there may be discrepancies due to misdiagnosis. In our study, many participants with chronic Lyme disease were also diagnosed with Chronic Fatigue Syndrome or fibromyalgia (Lantos, 2015). Our findings for Chronic Fatigue Syndrome differed from those of Gottschalk et al., with a notable difference being that Gottschalk et al. used age and biologically sex matched pairs. Analysis of our results based on averages rather than matched samples might yield different conclusions.

4.9 Future directions

Future directions start with testing more samples of each post-infectious syndrome, especially those with a small sample size for confirmation of results. Another future study could investigate other post-infectious syndromes that weren't tested in this study, including long covid, as this was the unfinished plan for this study. There is overall very little research on the relation of *ATG13* gene to post-infectious syndromes, or other diseases and disorders, so further research on this connection will provide more insight into how ATG13 interacts with the immune system.

4.10 Conclusion

My results show that the *ATG13* gene is under expressed in some post-infectious syndromes, specifically multiple sclerosis and treated, fully recovered Lyme participants. Having this information can provide potential information for testing, treatment, and diagnosis of these debilitating conditions. Knowing the gene expression of ATG13 in various post-infectious syndromes provides information on the gap in knowledge, allowing for more opportunity to study other post-infectious syndromes and to use this for testing in the future.

References

Afari, N., & Buchwald, D. (2003). Chronic Fatigue Syndrome: A Review. *American Journal of Psychiatry*, *160*(2), 221–236. https://doi.org/10.1176/appi.ajp.160.2.221

Aronson, J. K., & Ferner, R. E. (2017). Biomarkers—A General Review. *Current Protocols in Pharmacology*, *76*(1), 9.23.1-9.23.17. https://doi.org/10.1002/cpph.19

Bjørnevik, K., Münz, C., Cohen, J. I., & Ascherio, A. (2023). Epstein–Barr virus as a leading cause of multiple sclerosis: mechanisms and implications. *Nature Reviews. Neurology, 19(3), 160-171.* https://doi.org/10.1038/s41582-023-00775-5

Bobe, J. R., Jutras, B. L., Horn, E. J., Embers, M. E., Bailey, A., Moritz, R. L., Zhang, Y., Soloski, M. J., Ostfeld, R. S., Marconi, R. T., Aucott, J., Ma'ayan, A., Keesing, F., Lewis, K., Ben Mamoun, C., Rebman, A. W., McClune, M. E., Breitschwerdt, E. B., Reddy, P. J., … Fallon, B. A. (2021). Recent Progress in Lyme Disease and Remaining Challenges. *Frontiers in Medicine*, *8*, 666554. https://doi.org/10.3389/fmed.2021.666554

Branch, N. S. C. and O. (2017, April 5). *Fibromyalgia*. National Institute of Arthritis and Musculoskeletal and Skin Diseases; NIAMS. https://www.niams.nih.gov/health-topics/fibromyalgia

Chang, Y.-Y., & Neufeld, T. P. (2009). An Atg1/Atg13 Complex with Multiple Roles in TOR-mediated Autophagy Regulation. *Molecular Biology of the Cell*, *20*(7), 2004–2014. https://doi.org/10.1091/mbc.e08-12-1250

Chinn, S., Caldwell, W., & Gritsenko, K. (2016). Fibromyalgia Pathogenesis and Treatment Options Update. *Current Pain and Headache Reports*, *20*(4), 25. https://doi.org/10.1007/s11916-016-0556-x

Choutka, J., Jansari, V., Hornig, M., & Iwasaki, A. (2022a). Unexplained post-acute infection syndromes. *Nature Medicine*, *28*(5), Article 5. https://doi.org/10.1038/s41591-022-01810-6

Chronic Lyme Disease | NIAID: National Institute of Allergy and Infectious Diseases. (2018, November 21). https://www.niaid.nih.gov/diseases-conditions/chronic-lyme-disease

Dobson, R., & Giovannoni, G. (2019). Multiple sclerosis – a review. *European Journal of Neurology*, *26*(1), 27–40. https://doi.org/10.1111/ene.13819

Drexler, M., & Medicine (US), I. of. (2010). How Infection Works. In *What You Need to Know About Infectious Disease*. National Academies Press (US). https://www.ncbi.nlm.nih.gov/books/NBK209710/

Faissner, S., & Gold, R. (2019). Progressive multiple sclerosis: Latest therapeutic developments and future directions. *Therapeutic Advances in Neurological Disorders*, *12*, 1756286419878323. https://doi.org/10.1177/1756286419878323

Ghasemi, N., Razavi, S., & Nikzad, E. (2017). Multiple Sclerosis: Pathogenesis, Symptoms, Diagnoses and Cell-Based Therapy. *Cell Journal (Yakhteh)*, *19*(1), 1–10.

Gottschalk, G., Peterson, D., Knox, K., Maynard, M., Whelan, R. J., & Roy, A. (2022). Elevated ATG13 in serum of patients with ME/CFS stimulates oxidative stress response in microglial cells via activation of receptor for advanced glycation end products (RAGE). *Molecular and Cellular Neurosciences*, *120*, 103731. https://doi.org/10.1016/j.mcn.2022.103731

Harrison, D. A. (2012). The JAK/STAT Pathway. *Cold Spring Harbor Perspectives in Biology*, *4*(3), a011205. https://doi.org/10.1101/cshperspect.a011205

Hauser, S. L., & Cree, B. A. C. (2020). Treatment of Multiple Sclerosis: A Review. *The American Journal of Medicine*, *133*(12), 1380-1390.e2. https://doi.org/10.1016/j.amjmed.2020.05.049

Häuser, W., Ablin, J., Fitzcharles, M.-A., Littlejohn, G., Luciano, J. V., Usui, C., & Walitt, B. (2015). Fibromyalgia. *Nature Reviews Disease Primers*, *1*(1), Article 1. https://doi.org/10.1038/nrdp.2015.22

Hieke, N., Löffler, A. S., Kaizuka, T., Berleth, N., Böhler, P., Drießen, S., Stuhldreier, F., Friesen, O., Assani, K., Schmitz, K., Peter, C., Diedrich, B., Dengjel, J., Holland, P., Simonsen, A., Wesselborg, S., Mizushima, N., & Stork, B. (2015). Expression of a ULK1/2 binding-deficient ATG13 variant can partially restore autophagic activity in ATG13-deficient cells. *Autophagy*, *11*(9), 1471–1483. https://doi.org/10.1080/15548627.2015.1068488

Holgate, Komaroff, Mangan, D, & Wessely, S. (2011). *Chronic fatigue syndrome: Understanding a complex illness | Nature Reviews Neuroscience*. https://www.nature.com/articles/nrn3087

Kaizuka, T., & Mizushima, N. (2016). Atg13 Is Essential for Autophagy and Cardiac Development in Mice. *Molecular and Cellular Biology*, *36*(4), 585–595. https://doi.org/10.1128/MCB.01005-15

Karabi, Z., Moradian, F., & Kheirabadi, M. (2022). The effect of lactoferrin on ULK1 and ATG13 genes expression in breast cancer cell line MCF7 and bioinformatics studies of protein interaction between lactoferrin and the autophagy initiation complex. *Cell Biochemistry and Biophysics*, *80*(4), 795–806. https://doi.org/10.1007/s12013-022-01097-x

Kawamata, T., Kamada, Y., Suzuki, K., Kuboshima, N., Akimatsu, H., Ota, S., Ohsumi, M., & Ohsumi, Y. (2005). Characterization of a novel autophagy-specific gene, ATG29. *Biochemical and Biophysical Research Communications*, *338*(4), 1884–1889. https://doi.org/10.1016/j.bbrc.2005.10.163

Lantos, P. M. (2015). Chronic Lyme Disease. *Infectious Disease Clinics of North America*, *29*(2), 325–340. https://doi.org/10.1016/j.idc.2015.02.006

Levine, B., & Kroemer, G. (2019). Biological Functions of Autophagy Genes: A Disease Perspective. *Cell*, *176*(1–2), 11–42. https://doi.org/10.1016/j.cell.2018.09.048

Li, X., He, S., & Ma, B. (2020). Autophagy and autophagy-related proteins in cancer. *Molecular Cancer*, *19*(1), 12. https://doi.org/10.1186/s12943-020-1138-4

Merkling, S. H., Bronkhorst, A. W., Kramer, J. M., Overheul, G. J., Schenck, A., & Rij, R. P. V. (2015). The Epigenetic Regulator G9a Mediates Tolerance to RNA Virus Infection in Drosophila. *PLOS Pathogens*, *11*(4), e1004692. https://doi.org/10.1371/journal.ppat.1004692

Poenaru, S., Abdallah, S. J., Corrales-Medina, V., & Cowan, J. (2021). COVID-19 and post-infectious myalgic encephalomyelitis/chronic fatigue syndrome: A narrative review. *Therapeutic Advances in Infectious Disease*, *8*, 20499361211009385. https://doi.org/10.1177/20499361211009385

Raveendran, A. V., Jayadevan, R., & Sashidharan, S. (2021). Long COVID: An overview. *Diabetes & Metabolic Syndrome: Clinical Research & Reviews*, *15*(3), 869–875. https://doi.org/10.1016/j.dsx.2021.04.007

Sarzi-Puttini, P., Giorgi, V., Marotto, D., & Atzeni, F. (2020). Fibromyalgia: An update on clinical characteristics, aetiopathogenesis and treatment. *Nature Reviews Rheumatology*, *16*(11), 645–660. https://doi.org/10.1038/s41584-020-00506-w

Sellner, J., Kraus, J., Awad, A., Milo, R., Hemmer, B., & Stüve, O. (2011). The increasing incidence and prevalence of female multiple sclerosis—A critical analysis of potential environmental factors. *Autoimmunity Reviews*, *10*(8), 495–502. https://doi.org/10.1016/j.autrev.2011.02.006

Sherif, Z. A., Gomez, C. R., Connors, T. J., Henrich, T. J., & Reeves, W. B. (n.d.). Pathogenic mechanisms of post-acute sequelae of SARS-CoV-2 infection (PASC). *eLife*, *12*, e86002. https://doi.org/10.7554/eLife.86002

Siracusa, R., Paola, R. D., Cuzzocrea, S., & Impellizzeri, D. (2021). Fibromyalgia: Pathogenesis, Mechanisms, Diagnosis and Treatment Options Update. *International Journal of Molecular Sciences*, *22*(8), Article 8. https://doi.org/10.3390/ijms22083891

Stephan, J. S., Yeh, Y.-Y., Ramachandran, V., Deminoff, S. J., & Herman, P. K. (2009). The Tor and PKA signaling pathways independently target the Atg1/Atg13 protein kinase complex to control autophagy. *Proceedings of the National Academy of Sciences*, *106*(40), 17049–17054. https://doi.org/10.1073/pnas.0903316106

Wolfe, N. D., Dunavan, C. P., & Diamond, J. (2012). ORIGINS OF MAJOR HUMAN INFECTIOUS DISEASES. In *Improving Food Safety Through a One Health Approach: Workshop Summary*. National Academies Press (US). https://www.ncbi.nlm.nih.gov/books/NBK114494/

Wong, K. H., Shapiro, E. D., & Soffer, G. K. (2022). A Review of Post-treatment Lyme Disease Syndrome and Chronic Lyme Disease for the Practicing Immunologist. *Clinical Reviews in Allergy & Immunology*, *62*(1), 264–271. https://doi.org/10.1007/s12016-021-08906-w

Wu, Y., Liu, G., Li, Z., Chen, M., & Wang, Q. (2023). ATG13 is involved in immune response of pathogen invasion in blood clam Tegillarca granosa. *Frontiers in Veterinary Science*, *10*. https://doi.org/10.3389/fvets.2023.1141284

Yang, N., Hu, N., Zhang, J., Yi, J., Wang, Z., Wang, Y., Wu, P., & Chen, C. (2022). Bta-miR-2904 inhibits bovine viral diarrhea virus replication by targeting viral-infection-induced autophagy via ATG13. *Archives of Virology*, *168*(1), 11. https://doi.org/10.1007/s00705-022-05630-4

Yong, S. J. (2021). Long COVID or post-COVID-19 syndrome: Putative pathophysiology, risk factors, and treatments. *Infectious Diseases*, *53*(10), 737–754. https://doi.org/10.1080/23744235.2021.1924397

Appendix

A.1 Bioinformatics scan for allele frequencies

A bioinformatics scan for allele frequencies was conducted, looking for single nucleotide polymorphisms (SNPs) within the *ATG13* gene, but results showed that the SNPs were not common enough in the North American population, so this approach was abandoned.

A.2 Primer design

For designing primers, previous literature and bioinformatics was used to produce primers specific to the gene, *ATG13*. Primers were sourced, in part, from Karabi et al., 2022. The *ATG13* gene sequence (accession number: NM 001142673) that contained the forward primer was sourced from GenBank, then Primer Blast was used to generate the final forward and reverse primers, selecting the one with the shortest product length (4145 base pairs) and a low self-complementary value. These primers were not used, however, when the RNA approach was abandoned.

A.3 RNA extraction

Blood for RNA extraction was collected from cows (*Bos taurus*) as described in McGowan, 2019 (CACC #102183). RNA extraction was conducted following the RNeasy protocol (HB-0435-007_HB_RNYMini_0623_WW.pdf). To begin RNA extraction, the following items were sterilized and transferred into the fume hood (Labconco, protector laboratory hood E.FH31.EF6) using decontamination solution, water, and 70% ethanol as sterilization techniques: tubes, tube racks, pen, pipettes, labeled tubes, Qiagen RNA extraction kit (Lot #: 174022016, Ref #: 74004) supplies, scoopula, pestles, betamercaptoethanol, and tips. The empty tubes were weighed and then blood samples were distributed into the tubes and weighed to calculate how much blood was being used. Less than 20uL was the preferred amount. 600uL of RLT buffer (Lot #:175016067) (or 350uL if less than 20uL of blood used) multiplied by the number of samples used, plus 10uL of betamercaptoethanol (Lot #: SHBF0646V) per 1mL of RLT was measured out and placed into a collection tube provided by the RNA extraction kit.

Sample calculation for RNA extraction with six samples:

600uL RLT buffer x 6 samples = 3600 uL RLT buffer

3600 uL RLT buffer/3 (put into three tubes) = 1200 uL RLT buffer per tube

For betamercaptoethanol (very important to do this in a fume hood – toxic!):

3600uL RLT buffer/10uL = 360uL betamercaptoethanol

360uL betamercaptoethanol/3 = 120uL betamercaptoethanol per tube

Either 600uL or 350uL of RLT betamercaptoethanol mixture was placed into each blood sample, depending on how much blood was used (600uL for >20uL of blood, 350uL for <20uL of blood). Then a pestle was used to break apart the blood and mix it around. This mixture was then centrifuged (Spectrafuge 24D Labnet International Inc.; serial number: D103200) for three minutes at full speed (13,300 rpm). Once centrifuged, a pellet was observed at the bottom of the tube and the supernatant was pipetted out from each tube and put into a new sterile tube and the tube with the pellet was discarded into biohazardous waste. The same amount of ethanol as the supernatant was added to each tube and then mixed by pipetting. Quiagen columns (Lot #:166034101) were then labeled according to the corresponding samples then 700uL of the corresponding sample was transferred to the appropriate column. The old tubes were discarded. The columns were then centrifuged for 15 minutes at a speed of 10,000 rpm. The flow through was then discarded. 350uL of RWI buffer (Lot #:175020912) was added to the top of each column and was centrifuged for 15 seconds at a speed of 8000g and the flow through was poured out. 70uL of RDD buffer (Lot #: 145022315) multiplied by the number of samples was added to a new Eppendorf tube along with 10uL of DNAse stock solution multiplied by the number of samples. The Eppendorf tube was inverted to mix then centrifuged for 3 seconds. 80uL of the DNAse/RDD mixture was added to each column and allowed to sit for 15 minutes. Another 350uL of RWI buffer was added to the top of each column and was centrifuged for 15 seconds at a speed of 8000g. The flow through was discarded. 500uL of RPE buffer (Lot #: 175016202) was then added to each column and was centrifuged for 15 seconds at a speed of 8000g and the flow through was discarded. 500uL of RPE buffer was added a second time to the columns and was centrifuged for 2 minutes at a speed of 8000g. The flow through was discarded. The column was then centrifuged for 1 minute with a clean and sterile bottom attachment. Qiagen tubes were labeled according to the samples and the column was placed in the new tubes. 30uL of RNAse free H_20 (175016433) was added to each column and then was centrifuged for 1 minute at a speed of 8000g. The flow through was pipetting back into the column then centrifuged again to allow for an increased concentration. Approximately 3uL of this was set aside in a PCR tube for nano dropping the rest was immediately frozen. Samples were tested in a nanodrop (Nanodrop 1000). This method was no longer used when RNA was not found in the samples (shown below).

```
Sample ID       User ID Date    Time    ng/ul   A260    A280    260/280         260/230         Constant        Cursor Pos.
Cursor abs.     340 raw
DA31 RS Default 6/15/2023       1:06 PM -2.47   -0.062  -0.058  1.06    0.57    40.00   230     -0.108  -0.016
DA31 RS Default 6/15/2023       1:07 PM 2.08    0.052   0.001   37.00   0.02    40.00   230     2.413   -0.028
DA59 RS Default 6/15/2023       1:08 PM -0.04   -0.001  -0.008  0.12    0.00    40.00   230     1.070   0.096
DA17 RS Default 6/15/2023       1:09 PM 0.20    0.005   -0.019  -0.26   0.00    40.00   230     2.974   -0.015
DA45 RS Default 6/15/2023       1:09 PM -1.03   -0.026  -0.006  4.11    -0.10   40.00   230     0.265   0.019

Sample  ID      Curve Type      Ref  conc       Ref Abs Std 1 conc      Std 1 Abs.      Std 2 conc      Std 2 Abs       Std 3
conc    Std 3 Abs       Std 4 conc      Std 4 Abs       Std 5 conc      Std 5 Abs       Std 6 conc      Std 6 Abs       Std 7
conc    Std 7 Abs
DA31 RS         Interpolation
DA31 RS         Interpolation
DA59 RS Interpolation
DA17 RS Interpolation
DA45 RS Interpolation
```

Figure A.1. Results from nanodrop.